An Investigation of the Mechanism of the Rhodium-Catalyzed [5 + 1 + 2 + 1] Cycloaddition Reaction of Vinylcyclopropanes, Terminal Alkynes and Carbon-monoxide

By

Ifenna Irvin Mbaezue

A Thesis Submitted to

Saint Mary's University, Halifax, Nova Scotia

in Partial Fulfilment of the Requirements for

the Degree of Bachelor of Science

with Honours in Chemistry.

April 25th, 2017, Halifax, Nova Scotia

Supervisor: Dr. Kai E. O. Ylijoki

Chairperson of Chemistry Department: Dr. Robert D. Singer

Certification

An Investigation on the Mechanism of the Rhodium-Catalyzed [5 + 1 + 2 + 1] Cycloaddition Reaction of Vinylcyclopropanes, Terminal Alkynes and Carbon-monoxide

I hereby certify that this thesis was carried out by Ifenna Irvin Mbaezue in partial fulfilment for the requirements of the Degree of Bachelor of Science, Honours in Chemistry at Saint Mary's University. I certify that this is truly original work carried out by Ifenna Irvin Mbaezue.

An Investigation on the Mechanism of the Rhodium-Catalyzed [5 + 1 + 2 + 1] Cycloaddition Reaction of Vinylcyclopropanes, Terminal Alkynes and Carbon-monoxide

By

Ifenna Irvin Mbaezue

A Thesis Submitted to
Saint Mary's University, Halifax, Nova Scotia
in Partial Fulfillment of the Requirements for
the Degree of Bachelor of Science, Honours in Chemistry.

April 25th, 2017, Halifax, Nova Scotia

Approved: Supervisor
Dr. Kai E. O. Ylijoki

Approved: Chairperson
Dr. Robert D. Singer

Date: April 25th, 2017

An Investigation of the Mechanism of the Rhodium-Catalyzed [5 + 1 + 2 + 1] Cycloaddition Reaction of Vinylcyclopropanes, Terminal Alkynes and Carbon-monoxide

By

Ifenna Irvin Mbaezue

April 25th, 2017

Abstract

Spectroscopic investigations on the $[RhCl(CO)_2]_2$ catalysed [5 + 1 + 2 + 1] cycloaddition of VCP, CO and 4-ethynylbiphenyl[1] were performed and the existence of an off-cycle species was revealed. This species that forms at high Rh-catalyst loading mitigates cycloadduct formation even at elevated temperatures and long reaction periods. Furthermore, the mechanism for the conversion of the inactive species to an active species was hypothesised, as informed by previous computational studies. The starting material for the spectroscopic study, VCP, was synthesised by a modified procedure.[2] The reaction of 2-methoxyethanol with 1,3-butadiene in toluene was followed by the isolation of the resulting brominated intermediate. Subsequently, purification of the intermediate, followed by an elimination reaction afforded 2-(2-methoxyethoxy)-1,3-butadiene. A modified vacuum distillation method was used to purify the diene and subsequently, TLC monitored Simmons-Smith cyclopropanation was performed on the diene. The resulting VCP was also purified by the same method employed for the diene.

1. Wender, P. A.; Gamber, G. G.; Hubbard, R. D.; Pham, S. M.; Zhang, L. *J. Am. Chem. Soc.* **2005**, 127, 2836.

2. Wender, P. A.; Dyckman, A, J.; Husfeld, C. O.; Scanio, M. J. C. *Org. Lett*. **2000**, 2, 1609.

Acknowledgements

Firstly, I would like to thank my supervisor, Prof. Kai E. O. Ylijoki, for this opportunity. Through this work, I have developed a keen appreciation and interest in the synergistic combination of synthetic, spectroscopic, and computational chemistry. As a result of Prof. Ylijoki's guidance and expertise, my skills in numerous facets of chemistry have appreciably developed.

To you my parents, Uche and Nkwute, and my siblings, Chi, Ugo and Chu, for your sacrifices and support. I would be lost without you.

I would also like to thank Aiden and Alison for being wonderful.

Table of Contents

List of Symbols and Abbreviations

atm	atmosphere
$CDCl_3$	deuterated chloroform
CO	carbon monoxide
cod	1,5-cyclooctadiene
COSY	correlation spectroscopy
DEPT-Q	distortion Enhancement by polarisation transfer quaternary
DFT	Density Functional Theory
EtOAc	ethyl acetate
equiv.	equivalent
Fig.	Figure
HOMO	highest occupied molecular orbital
HSQC	heteronuclear single quantum correlation spectroscopy
INT	intermediate
LUMO	lowest unoccupied molecular orbital
NBS	N-bromosuccinimide
NMR	nuclear magnetic resonance
TLC	thin layer chromatography
TS	transition state

toluene-d_8	deuterated toluene
VCP	1-(2-methoxyethoxy)-1-vinylcyclopropane

List of Schemes

List of Figures

1. Introduction

1.1 Cycloaddition Reactions

Pericyclic reactions are a broad class of reactions that involve the concerted breakage and formation of bonds.[1] These reactions proceed via conjugated transition states that are stabilized by delocalised pi-bonds.[1] While the nature of solvents used in pericyclic reactions does not affect the reaction rates by a substantial degree, these reactions can be fostered by photochemical and thermal factors.[1] In addition, pressurized conditions enable the formation of condensed transition states with a negative activation volume when compared to the preceding bimolecular state.[1] Hence, pressurized conditions also affect pericyclic reaction rates while enabling the favourable formation of transition states.

Cycloaddition reactions are a subgroup of pericyclic reactions that can be employed in the synthesis of cycloadducts, via cyclic transition states and the formation of new sigma bonds.[1] These concerted reactions are promoted by the phase matched interactions of the HOMO of an unsaturated reactant, with the LUMO of another reactant.[1] Cycloaddition reactions are usually represented as [m + n] additions, where 'm' and 'n' refer to the number of atoms that are involved in the reaction. While suprafacial additions are cycloaddition reactions that occur across the same side of the pi-system, antarafacial additions occur across opposite sides of the pi-system.[1]

A classic and powerful example of a cycloaddition reaction is the [4 + 2] Diels-Alder reaction,[2] whereby the 4-carbon unit of a diene reacts with the 2-carbon unit of a dienophile, to yield a 6-membered cycloadduct.

1.2 Rhodium in Cycloaddition Chemistry

Transition metal catalysed cycloaddition reactions have provided a wide array of synthetic possibilities because metal catalysts allow the complexation of the metal to an olefin or alkyne, leading to enhanced reactivity.[3] As a result of the versatility of cycloaddition reactions, numerous methods have been developed for the synthesis of rings having varying numbers of carbon atoms. It is pertinent to note that while such reactions are formally considered as cycloadditions, they proceed in a stepwise fashion instead of a concerted manner.

Rhodium has catalysed the synthesis of numerous ring compounds, ranging in size from 3- to 9-membered cycloadducts. The versatility of this metal as a catalyst results from its variable oxidation state as well as its ability to form coordinate bonds with an array of ligands. Thus, through low energy coordination and insertion steps, rhodium has found invaluable use in the catalysis of numerous mechanistic cycles.[4]

Herein, Rh-catalysed cycloaddition reactions are presented and key mechanistic pathways are discussed. Scheme 1.1 portrays a summary of these reactions, while depicting the robust catalytic nature of rhodium in cycloaddition chemistry.

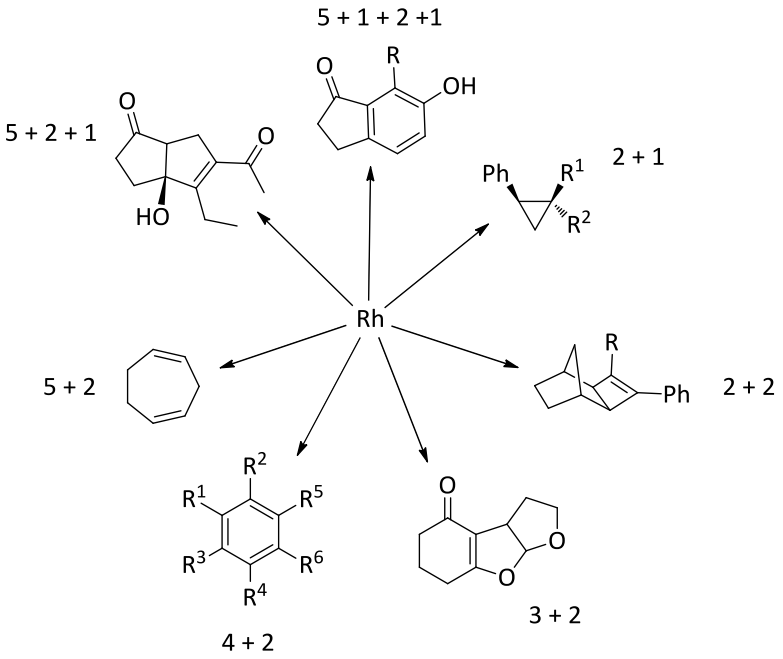

Scheme 1.1: Rh-catalysed cycloaddition reactions in the synthesis of a wide array of rings.

1.2.1 Rh-catalysed [2 + 1] cycloaddition reactions in the synthesis of 3-membered rings

1.2.1.1 Alkyl carbenes in [2 +1] cycloaddition

When metals such as Rh are in the presence of diazoalkanes, transition metal-carbene intermediates are formed.[3] In 1984, Doyle and co-workers reported the $Rh_2(OAc)_4$-catalysed [2 + 1] cyclopropanation reaction involving phenyldiazomethane and various olefins (Scheme 1.2).[5] In each reaction, ethyl ether was the solvent of choice and a large excess of the olefin was used. It was discovered that the nucleophilic property of the olefin highly influenced the nature of the catalytic cycle involved in phenylcyclopropane synthesis. Although E/Z-mixtures of the cyclopropanes were usually obtained, the formation of the (Z)-isomer was favoured in some instances.

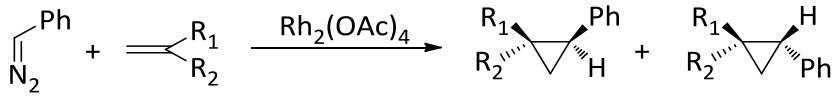

Scheme 1.2: Rh-catalysed cyclopropanation of phenyldiazomethane and olefins.[5]

The mechanism proposed by Doyle highlights this preferential formation of the (Z)-isomer (Scheme 1.3). The association of the electrophilic metal carbene **1** with the olefin **2** via path A, affords the π-complex **3**. Afterwards, the backside displacement of the metal centre via the carbenium ion **4** yields the less sterically hindered (Z)-isomer **5**. Through path B, the more sterically hindered π-complex **6** is afforded. Subsequently, metal displacement via the carbenium ion **7** yields the more sterically hindered (E)-isomer **8**.[3, 5, 6] Thus, it is apparent that minimal steric hindrance is a major factor in the preferential formation of the (Z)-isomer.

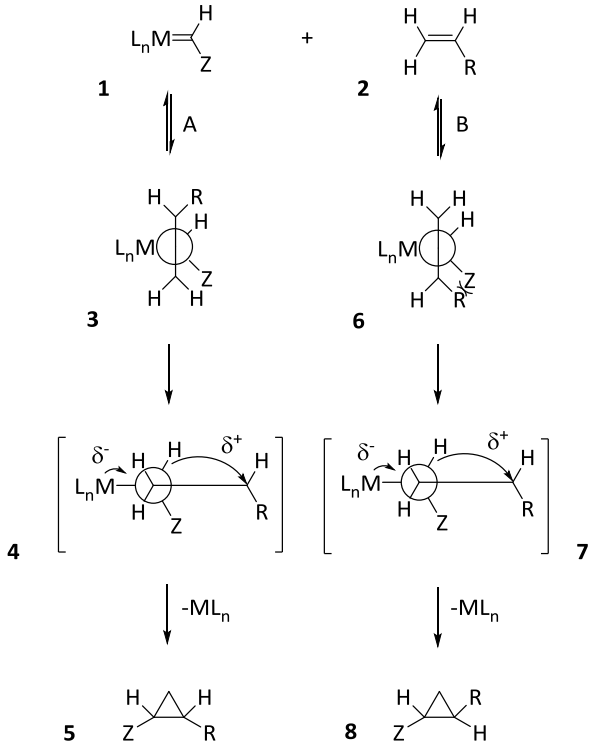

Scheme 1.3: Mechanism of the Rh-catalysed cyclopropanation of phenyldiazomethane and olefins.[3, 5, 6]

1.2.1.2 Vinylcarbenes in [2 + 1] cycloaddition reactions

The metal catalysed synthesis of 3-membered rings is not limited to the use of alkyl carbenes alone. In 1975, Salomon and co-workers reported the first cycloaddition reaction of vinylcarbenes in the syntheses of vinylcyclopropanes, via the Cu-catalysed reaction of olefins with vinyldiazomethane.[7] In 1991, the application of Rh-vinylcarbenes to cyclopropanation was reported by Padwa and co-workers.[8] Via the reaction of o-alkynyl-substituted α-diazoacetophenones with Rh(II) carboxylates, the Padwa group synthesised various substituted indenones through cyclopropanation. Metallacyclobutenes resulting from the complexation of vinylcarbenes with transition metals may undergo rearrangements and as such, elicit unexpected cycloaddition reaction pathways.[3] Hence, the mechanism proposed by Padwa and co-workers is quite intricate: the addition of the Rh-carbenoid to the acetylenic σ-bond forms the vinyl carbenoid **10** either through the metallacyclobutene intermediate **9**, or via the strained cyclopropene **11**. Subsequent addition of **10** to the tethered alkene yields the indenone (Scheme 1.4).[8]

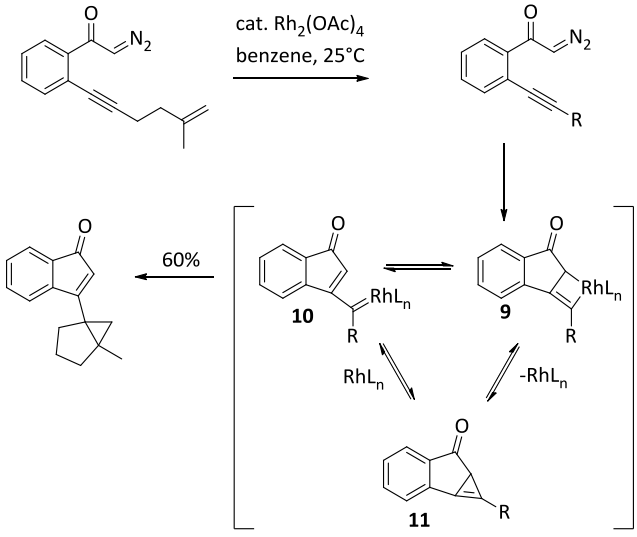

Scheme 1.4: Mechanism of indenone synthesis via a Rh-vinylcarbene Intermediate.[8]

1.2.2 Rh-catalysed [2 + 2] cycloaddition in the synthesis of 4-membered rings

Rhodium catalysis has been extended to the synthesis of 4-membered rings via [2 + 2] cycloadditions. In addition to its catalytic role in such reactions, a chiral rhodium catalyst can introduce stereochemistry into cyclobutene products. In 2006, Shibata and co-workers reported the enantioselective Rh-catalysed [2 + 2] cycloaddition of norbornene derivatives and alkynyl esters, in the syntheses of chiral cyclobutenes (Scheme 1.5).[9] In this unprecedented work that employed the chiral catalyst [Rh(cod)(H_8-binap)]BF_4, it was discovered that the electron deficient substituent at the alkyne terminus fostered the cycloaddition. In addition, the etheric oxygen was shown to play an important role in asymmetric induction.[9] While tert-butyl and benzyl esters resulted in reduced enantioselectivity, alkynyl ketone gave a high-yielding cycloadduct of poor enantiomeric excess.[9]

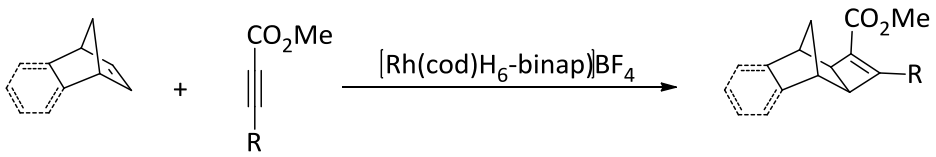

Scheme 1.5: Rh-catalysed synthesis of chiral cyclobutenes.[9]

1.2.3 Rh-catalysed cycloaddition reactions in the synthesis of 5-membered rings

Various Rh-catalysed reactions have been designed towards the synthesis of 5-membered rings. These reactions either entail the cycloaddition of two components as seen in [3 + 2] and [4 + 1] cycloadditions, or involve the cycloaddition of three components as seen in [2 + 2 + 1] cycloaddition reactions.

1.2.3.1 Rh-catalysed [3 + 2] cycloaddition

Metal carbenoids such as the Zn-carbenoid employed by Simmons and Smith,[10] have provided ready access to the synthesis 3-membered rings. However, while such

carbenoids are commonly used in cyclopropanation reactions, Rh-carbenoids have been shown to afford 5-membered rings. In 1991, Piurrung and co-workers performed a $Rh_2(OAc)_4$ catalysed reaction of diazodimedone **12** and furan to yield the tricyclic product **16** (Scheme 1.6).[11]

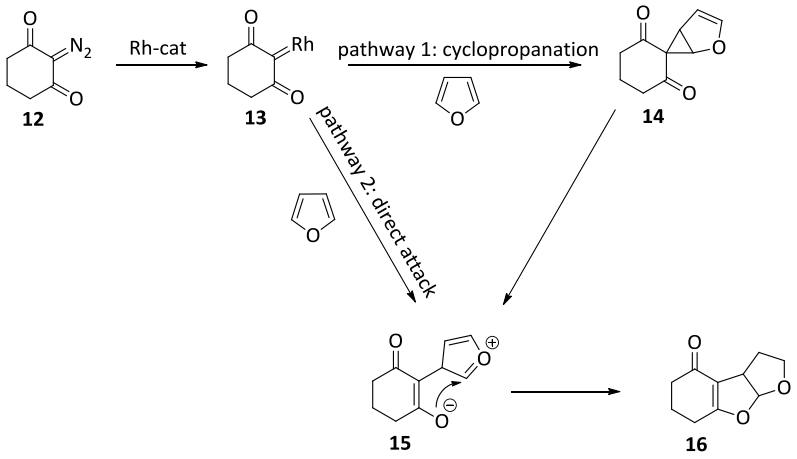

Scheme 1.6: Mechanism of the Rh-catalysed [3 + 2] cycloaddition reaction of diazodimedone and furan.[11]

Two mechanistic pathways have been proposed for this reaction (Scheme 1.6). In the first pathway, the reaction of Rh-carbenoid **13** and the furan yields the cyclopropane intermediate **14**, which undergoes fragmentation to yield the zwitterion **15**. Subsequent nucleophilic attack of the positively charged furan ring by the anionic oxygen yields the tricyclic compound **16.** In the second pathway, the direct attack of the furan on the Rh-carbenoid **13** yields the product **16** via the zwitterion **15**, without the formation of the cyclopropane intermediate **14**. [3,11] The difficulty in isolating such cyclopropane intermediates as well as the inability to convert these intermediates to the corresponding furans, when intermediate isolation was possible, corroborates the existence of the second mechanistic pathway.[12] A more recent example of a novel [3 + 2] cycloaddition, is the Rh(I)-catalysed synthesis of cyclopentadienones using cyclopropenones and

alkynes, performed by Wender and co-workers in 2006 (Scheme 1.7).[13] The controlled nature of this reaction allows high regioselectivity and synthetic efficiency.

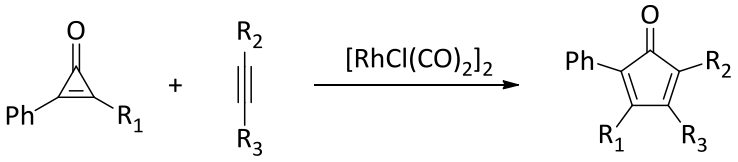

Scheme 1.7: Rh-catalysed cycloaddition of cyclopropenones and alkynes in the synthesis of cyclopentadienones.[13]

1.2.3.2 Rh-catalysed [2 + 2 + 1] cycloaddition

Metal-catalysed Pauson-Khand reactions have provided a robust route to the synthesis of substituted cyclopentenones.[14] Among the transition metals used in these reactions, rhodium has been routinely employed in the synthesis of such cycloadducts. In 1998, Koga and co-workers reported that the [2 + 2 + 1] intramolecular Pauson-Khand cycloaddition of 1,6-enynes and CO (1 atm) can be catalysed by $[RhCl(CO)_2]_2$, to yield various bicyclic cyclopentenones.[15] In the same year, Jeong and co-workers reported that while $RhCl(PPh_3)_3$ and *trans*-$RhCOCl(PPh_3)_2$ required an initial activation of AgOTf to catalyse this reaction, trans-$[RhCl(CO)(dppp)]_2$ required no activation to catalyse the [2 + 2 + 1] cycloaddition (Scheme 1.8).[16]

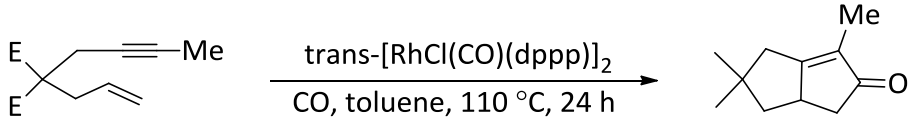

Scheme 1.8: Rh-catalysed cycloaddition of 1,6-enynes and CO.[16]

The versatility of rhodium has allowed many more novel Pauson-Khand cycloadditions, such as the intermolecular carbonylate [2 + 2 + 1] cycloaddition of alkynes, where alcohols serve as the CO source.[17]

1.2.3.3 Rh-catalysed [4 + 1] cycloaddition

A year after Koga's publication, Murakami and co-workers reported the synthesis of various (vinylallene)rhodium complexes (using $RhCl(PPh)_3$), which exhibited η^2, η^4 and σ^2-coordination to the metal centre.[18] The fluxionality exhibited by the η^4-complex, as well as the stable, planar nature of the σ^2-complex suggested a significant contribution of metallacyclic intermediates. These researchers reasoned that the migratory insertion of CO into the C-Rh σ-bond of the rhodacyclo-3-pentene intermediate **18**, could result in the incorporation of CO into the diene framework, to afford the [4 + 1] cycloadduct.[18] These hypotheses fostered their venture into a series of Rh-catalysed [4 + 1] vinylallene-CO cycloadditions. When the (η^4-vinylallene)rhodium complex **17** was stirred in dichloromethane under 1 atmosphere of CO, the [4 + 1] cycloaddition proceeded to afford the 2-(alkylidene)cyclopent-3-en-1-one product. A proposed mechanism for this reaction involves the coordination of CO to the metal centre of complex **18**, to yield the (vinylallene)carbonylrhodium species **19**. It should be noted that the (η^4-vinylallene)rhodium complex **17** is in equilibrium with the rhodacyclo-3-pentene intermediate **18.** Subsequently, the migratory insertion of CO into the σ C-Rh bond of **18** (via the coordination complex **19**), followed by reductive elimination, yields the [4 + 1] cycloadduct **20** (Scheme 1.9).[18]

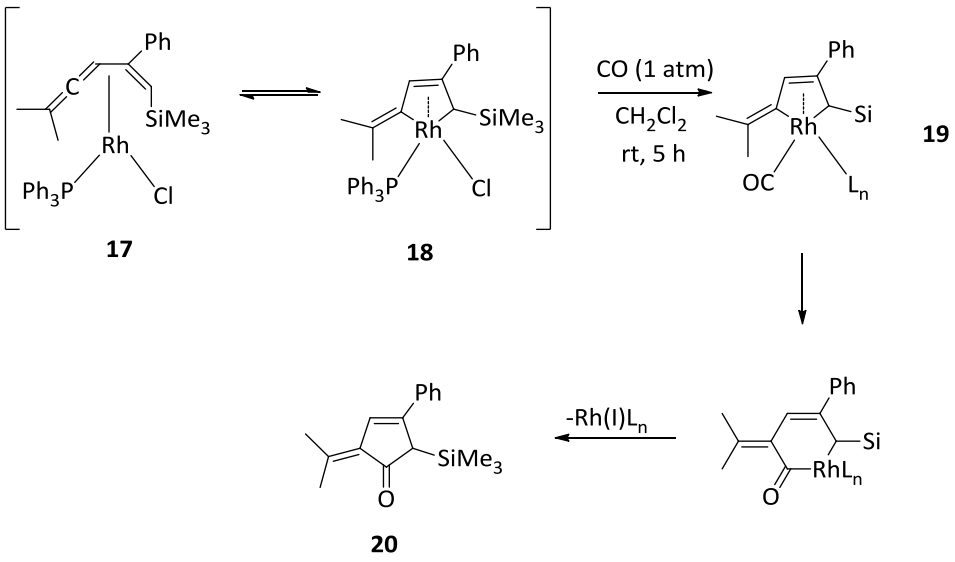

Scheme 1.9: Mechanism of the Rh-catalysed [4 + 1] cycloaddition of vinylallenes and CO.[18]

Rh-catalysed [4 + 1] cycloadditions have since then enabled the syntheses of other novel compounds such as pyrrole derivatives.[19]

1.2.4 Rh-catalysed cycloaddition reactions in the synthesis of 6-membered rings

1.2.4.1 Rh-catalysed [2 + 2 + 2] cycloaddition

Transition metals such as rhodium have enabled the evasion of entropic barriers to [2 + 2 + 2] cycloaddition reactions, via the step-wise and low energy coordination of reactants to the metal centre.[3] As a result, numerous reactions such as acetylene trimerization and acetylene-olefin trimerization have been achieved via metal catalysis.[3]

The cyclotrimerization of acetylene was optimized by Grigg and Stevenson: in the presence of [$RhCl(PPh_3)_3$], the cycloaddition of hepta-1,6-diynes and terminal unhindered monoalkynes readily afforded the [2 + 2 + 2] cycloadduct.[3,20,21] The proposed mechanism for these cyclotrimerization reactions involves the displacement of two ligands from the metal catalyst, by two alkyne units, to yield coordination

complex **21**. Subsequently, oxidative coupling yields the metallacyclopentadiene **22**, followed by the coordination and insertion of a third alkyne moiety. The resulting metallacycloheptatriene **23** or Diels-Alder adduct **24** then undergoes reductive elimination to yield the aromatic cycloadducts **25** (Scheme 1.10).[3,21,22]

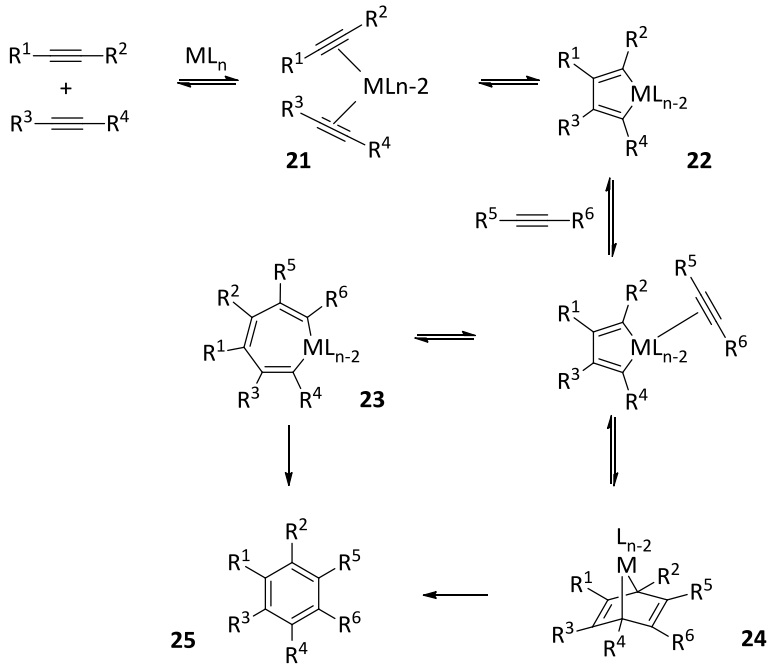

Scheme 1.10: Mechanism of the transition metal-catalysed [2 + 2 + 2] cyclotrimerization of alkynes.[3,21,22]

1.2.4.2 Rh-catalysed [4 + 2] cycloaddition

Diels-Alder reactions[2] are one of the most robust and versatile cycloaddition reactions. Thus, the incorporation of transition metal chemistry in the synthesis of [4 + 2] cycloadducts has allowed for an even broader accessibility to novel 6-membered rings. A quintessential Rh-catalysed [4 + 2] cycloadditions is the $[Rh(cod)(dppb)]^+$ catalysed cycloaddition of dienes and terminal alkynes (Scheme 1.11).[23]

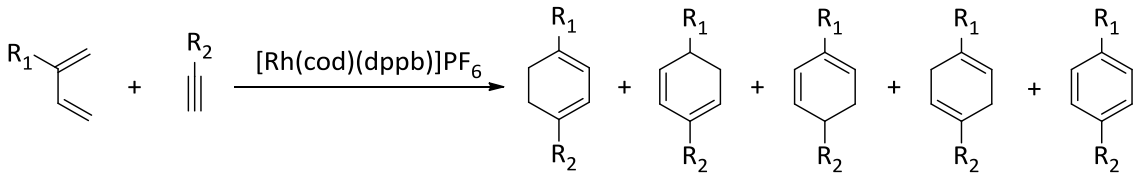

Scheme 1.11: Rh-catalysed cyclo-codimerization in the synthesis of cyclohexadienes.[23]

In 1995, the Wender group reported a novel transition metal-catalysed intramolecular [4 + 2] cycloaddition of dienes and allenes, in the syntheses of 6,6- and 6,5-fused rings.[24] These researchers noticed that when the diene-allene **26** is treated with 10 mol% of $Ni(COD)_2$ and 30 mol% of $P(O\text{-}oBiPh)_3$ (Ni-route), the diene moiety added to the terminal allene π-system, to afford isomers **28a,b**. However, when **26** was treated with 5 mol% of $[RhCl(CO)_2]_2$ and 48 mol% of $P(O\text{-}oBiPh)_3$ (Rh-route), the reversal of chemoselectivity occurred to yield one stereoisomer of the hydrindane **27**.[24] A proposed mechanism for the Rh-catalysed pathway involves the coordination of the Rh-catalyst **29** to diene-allene **26**, to afford the Rh-allene **30**. Subsequent metal association with the diene affords complex **31** and oxidative addition yields the metallacyclopentane **32**. Afterwards, **32** undergoes rotational and positional isomerisation to yield complex **34**, via complex **33**. Reductive elimination affords Rh-coordinated cycloadduct **35** and subsequent metal dissociation yields the cycloadduct, **27** (Scheme 1.12).[24]

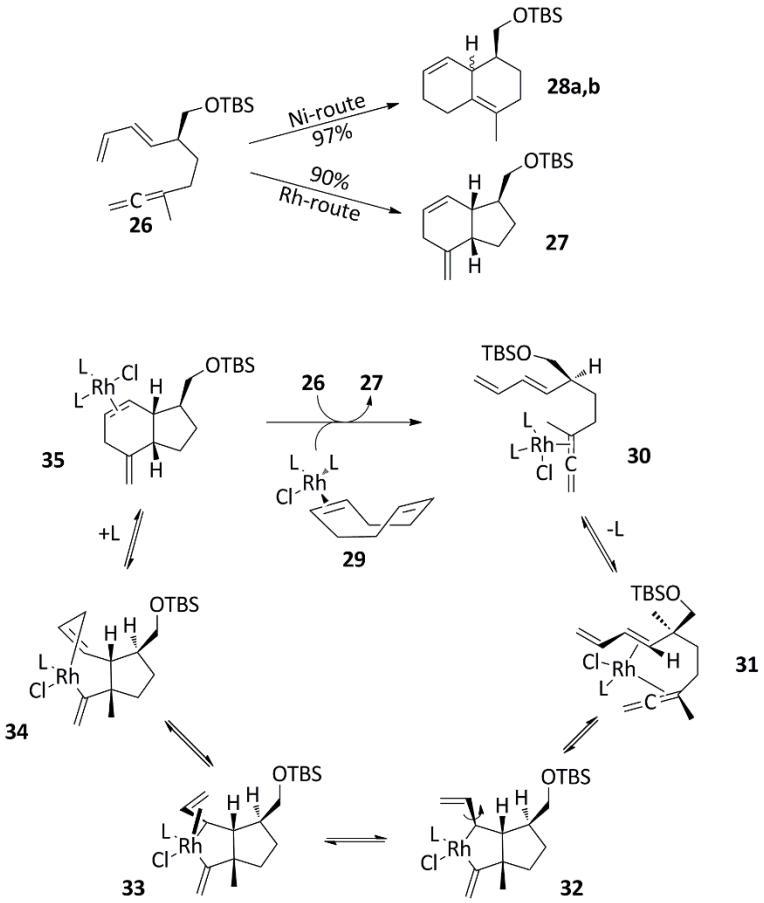

Scheme 1.12: Mechanism of the intramolecular Rh--catalysed [4 + 2] cycloaddition of dienes and allenes.[24]

However, prior to Wender's publication, Livinghouse and co-workers reported the low valent Rh-catalysed intramolecular cycloaddition of a tethered dienophile and diene.[25] In order to optimise the steric and electronic nature of the ligands attached to the Rh-centre, these researchers reacted various phosphine ligands with $[Rh(cyclooctene)_2]_2$ and assessed the effectiveness of the resulting compounds in the catalysis of [4 + 2] cycloadditions.[25] It was discovered that when d^8 Rh-complexes bearing 1,1,1,3,3,3-hexafluoro-2-propoxy phosphine ligands were employed, the efficacy of the Diels-Alder reaction was greatly improved. These catalysts provided low energy pathways that allowed the reaction to proceed at 25 °C.[25] A proposed mechanism for this Rh(I) catalysed Diels-Alder reaction is initiated by the addition of the metal to the tethered

complex **36**, to form the η^1-η^3 complex **37**. Subsequently, the metallacycle **38** is formed and reductive elimination yields the cycloadduct **39** (Scheme 1.13).[3,25,26]

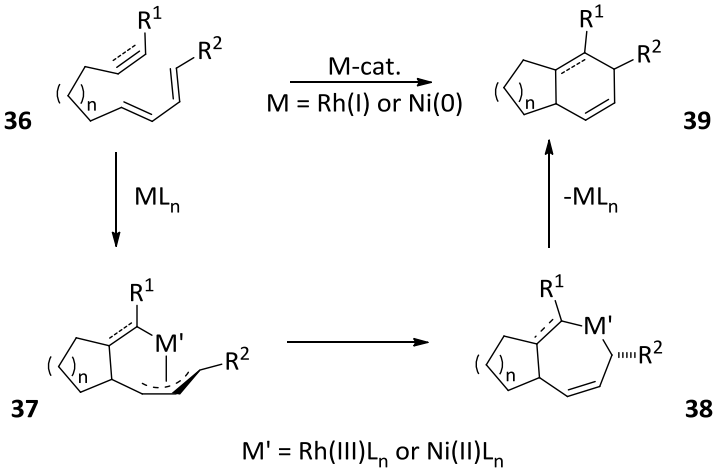

Scheme 1.13: Mechanism of the Rh-catalysed intramolecular [4 + 2] cycloaddition of a tethered dienophile and diene.[3,25,26]

1.2.4.3 Rh-catalysed [5 + 1] cycloaddition reactions

In addition to the [2 + 2 + 2] and [4 + 2] cycloaddition reactions described herein, [5 + 1] cycloadditions also provide a viable route to the synthesis of 6-membered rings. In 2010, Malacria and co-workers reported the first metal-catalysed [5 + 1] carbonylative cycloaddition of 3-acyloxy-1,4-enynes and CO.[27] Via this $[RhCl(CO)_2]_2$ catalysed reaction biologically active compounds such as resorcinols[28] can be readily synthesised. Although these researchers proposed a mechanism for this reaction, it was not until 2015 that Tang and co-workers reported a thorough DFT investigation of this reaction.[29] The Tang group proposed that the $[RhCl(CO)_2]_2$ catalyst dissociates and coordinates to the 3-acyloxy-1,4-enyne, to yield coordination complex **40**. Subsequently, 1,2-acyloxy migration affords complex **41**, followed by CO coordination to yield complex **42** and CO insertion to yield the 7-membered metallacycle **43**. Afterwards, **43** undergoes isomerisation to yield complex **44** followed by reductive elimination to yield the ketene

intermediate **45** and 6π-electrocyclization to yield carbocycle **46**. Finally, aromatization affords the resorcinol **47** (Scheme 1.14).[29]

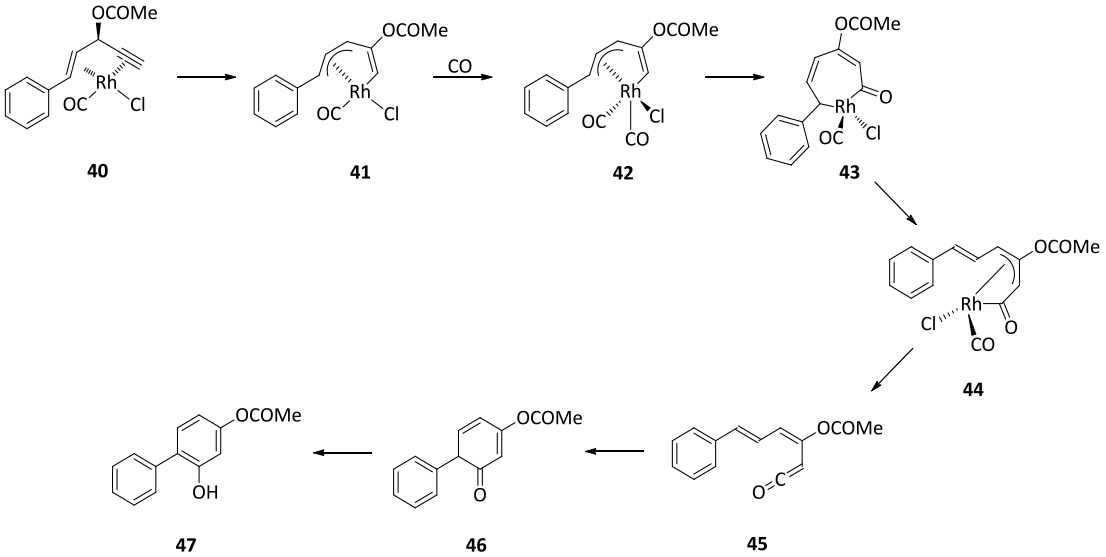

Scheme 1.14: Mechanism of the Rh-catalysed [5 + 1] cycloaddition of 3-acyloxy-1,4-enyne and CO.[29]

1.2.5 Rh-catalysed cycloaddition reactions in the synthesis of 7-membered rings

The high level of control (for example, via stereoselectivity) that metal-catalysed [5 + 2] cycloadditions afford, has enabled the synthesis of numerous substituted 7-membered rings.[1] In 1995, Wender and co-workers reported the first metal-catalysed [5 + 2] cycloaddition: the $[RhCl(PPh_3)]_3$ catalyzed intramolecular [5 + 2] cycloaddition of tethered vinylcyclopropanes and alkynes.[30] The basis for their venture into the discovery of this reaction was their hypothesis that a metallacycle is formed from the oxidative addition of the metal to the vinylcyclopropane and π-system. According to this hypothesis, the subsequent reductive elimination of the metal yields the 7-membered ring. Since this discovery, other novel Rh-catalysed [5 + 2] cycloadditions have been achieved. In addition, thorough mechanistic investigations have been used to elucidate the pathways of these reactions. Extensive DFT investigations[31] have

elucidated the mechanism of intermolecular $[RhCl(CO)_2]_2$ catalysed [5 + 2] cycloadditions of vinylcyclopropanes and alkynes. The proposed mechanism shows that the catalyst dimer dissociates to give the active $Rh(CO)_2Cl$ species. Subsequently, the coordination of this species to the vinylcyclopropane, with the subsequent loss of a CO from complex **48**, yields the 16-electron vinylcyclopropane-Rh(CO)Cl complex **49**. Further conformational changes followed by alkyne coordination (complex **50**), rate-determining insertion (complex **51**), and reductive elimination of the metal catalyst (complex **52**), yield the 7-membered cycloadduct **53** (Scheme 1.15).[1d, 31]

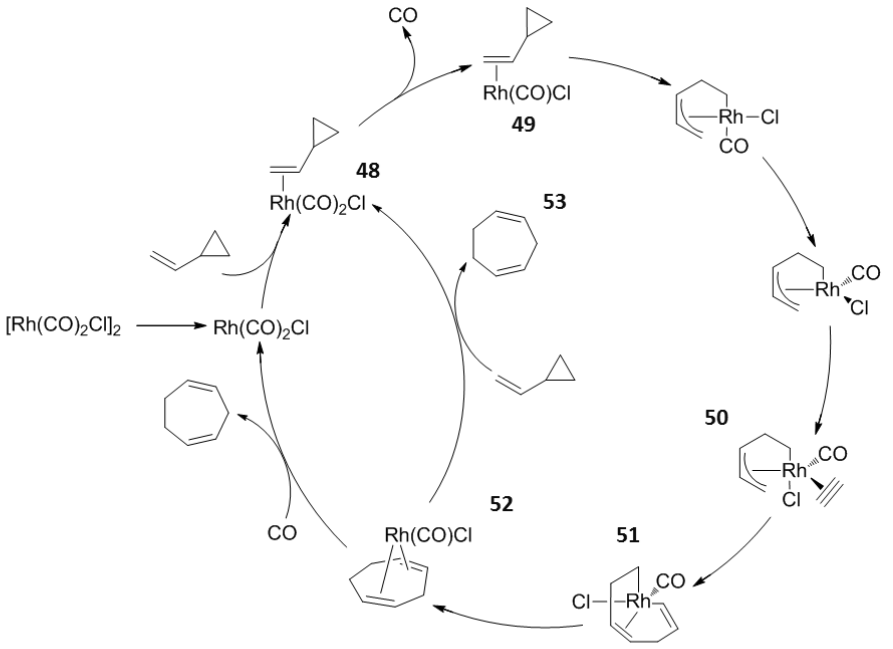

Scheme 1.15: Mechanism of the intermolecular Rh-catalysed [5 + 2] cycloaddition of vinylcyclopropanes and alkynes.[1d, 31]

It is noteworthy to mention that the mechanisms of other transition metal-catalysed [5 + 2] cycloadditions have also been extensively studied, for example, from the perspective of ligand control via [Ni(NHC)] catalysis[32], and selectivity in Ru(II) catalysis.[33]

Other examples of Rh-catalysed 7-membered ring forming reactions include Rh(I)-catalysed [4 + 3] cycloaddition reactions affording tropanes,[34] and bicyclo[5.3.0]decanes.[35]

1.2.6 Rh-catalysed cycloaddition reactions in the synthesis of 8-membered rings

Five years after their discovery of the metal-catalysed [5 + 2] cycloaddition, Wender and co-workers reported the first Rh(I)-catalysed [6 + 2] cycloaddition of 2-vinylcyclobutanones and alkenes, to afford cyclooctenones.[36] Initial trials that employed simple vinylcyclobutanes as the substrates, proved unsuccessful. However, the realisation that rhodium readily inserts into cyclobutenones,[37] in conjunction with previous success in the use of substituted substrates, prompted these researchers to employ vinylcyclobutanones. This reaction was optimized using 5 mol% $[RhCl(CO_2)]_2$, 10 mol% PPh_3 and 10 mol% of AgOTF to elicit the formation of the cycloadduct (Scheme 1.16).[36]

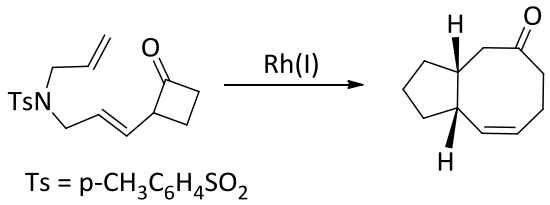

Scheme 1.16: The Rh(I)-catalysed [6 + 2] cycloaddition of vinylcyclobutanones and alkenes.[36]

Two years later, the Wender group reported the first metal catalysed [5 + 2 + 1] cycloaddition reaction. This $[RhCl(CO)_2]_2$ catalysed cycloaddition of vinylcyclopropanes, alkynes and CO, was employed in the synthesis of various bicyclo[3.3.0]octenone derivatives. Increased yields occurred at high CO pressure, 60 °C and interestingly, lower catalyst loading (Scheme 1.17).[38]

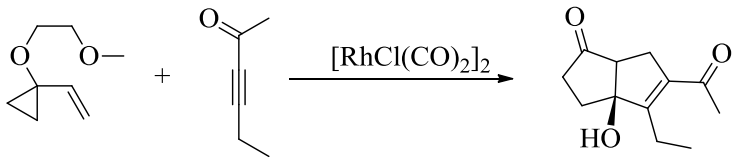

Scheme 1.17: The Rh(I)-catalysed [5 + 2 + 1] cycloaddition of vinylcyclopropanes, alkynes and CO.[38]

The Rh-catalysed [5 + 2 + 1] cycloaddition has found great use in the syntheses of numerous compounds. For instance, via the synergy of DFT studies and reaction design, natural 8-membered compounds such as (±)-asterisca-3(15),6-diene and (+)-asteriscanolide have been successfully synthesised.[39]

Other examples of 8-membered ring forming reactions include the Rh(I)-catalysed [4 + 2 + 2] cycloaddition of alkenes, alkynes and 1,3-dienes (Scheme 1.18).[40]

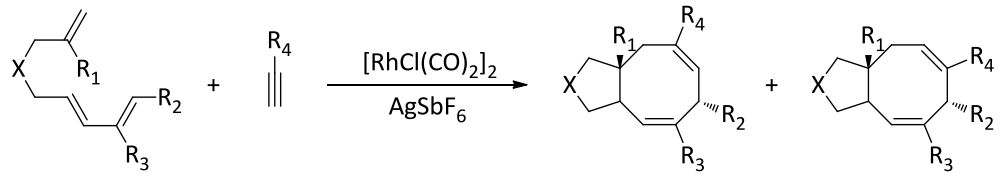

Scheme 1.18: Rh-catalysed synthesis of cyclooctadienes.[40]

1.2.7 Rh-catalysed synthesis of 9-membered rings: the [5 + 1 + 2 + 1] cycloaddition of VCP, alkynes and CO

In 2005, an unprecedented feat was achieved: the first 4-component, Rh-catalysed [5 + 1 + 2 + 1] cycloaddition reaction of VCP, CO and terminal alkynes was reported by Wender and co-workers.[41] The Wender group proposed a mechanism that entails the Rh-catalyzed cycloaddition of the 4 components (1 equivalent of VCP, 1 equivalent of a terminal alkyne and 2 equivalents of CO) to form a 9-membered intermediate **54**, that then undergoes tautomerization to form complex **55.** Subsequently, electrocyclization

affords bi-cyclic intermediate **56** and alcohol elimination yields the hydroxydihydroindanone **57** (Scheme 1.19).[41]

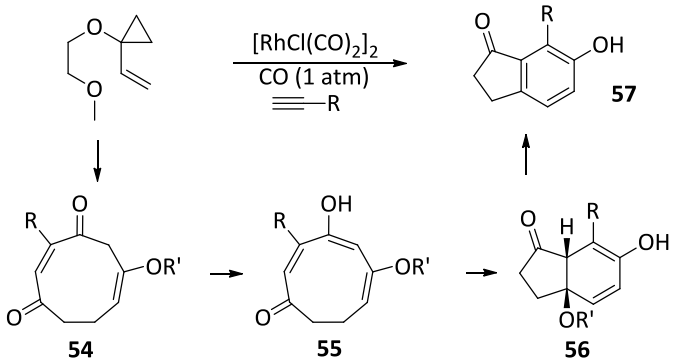

Scheme 1.19: The Rh-catalysed [5 + 1 + 2 + 1] cycloaddition of VCPs, terminal alkynes and CO.[41]

Indanones have a wide variety of uses, for instance, as precursors in the synthesis of potential monoamine oxidase (MAO) inhibitors,[42] as constituent building blocks of anticancer agents[43] and as reagents in the synthesis of antiviral drugs for treating bovine viral diarrhoea (BVD).[44] Despite the vast potential applications that indanones display, as well as the novelty of the [5 + 1 + 2 + 1] cycloaddition reaction and its robust applications in the synthesis of various substituted hydroxydihydroindanones, the mechanism of this reaction has not been previously investigated. Thus, we decided to elucidate the mechanistic pathway of the [5 + 1 + 2 + 1] cycloaddition reaction via computational methods, at the ωB97XD[45]/def2TZVPP[46] level of theory, with DFT calculations performed via the Gaussian09 (Revision C.01) software suite.[47] Our calculations revealed the existence of two competing cycloaddition pathways: the [5 + 1 + 2 + 1] and the [5 + 1 + 1 + 2] manifolds. In addition, we discovered that alkyne insertion was rate determining in both pathways in accordance with the [5 + 2] mechanism.[31] In the effort to gain further insight into the complex nature of both pathways, understand the rationale for the high-energy alkyne insertion barriers we had

obtained, as well as further elucidate the on-metal cyclization and aromatization phases we predicted, I embarked on a spectroscopic study of this reaction, as reported in this thesis. NMR Spectroscopy is an invaluable tool, pertinent in the elucidation of molecular structures as well as in the investigation of mechanistic pathways. While ^{103}Rh NMR[48] has been employed in the elucidation of the mechanism of rhodium-catalyzed reactions such as the Rh-catalyzed oxidative carbonylation of toluene to toluic acid,[49] our investigation of the [5 + 1 + 2 + 1] cycloaddition reaction will initially rely on the analyses of resulting 1D and 2D ^{1}H NMR and ^{13}C NMR spectra. Subsequent experiments may require ^{103}Rh NMR in the spectroscopic elucidation of the metal mediated cyclization and aromatization phases that we have proposed.

The elucidation of the [5 + 1 + 2 + 1] cycloaddition is pertinent to the understanding of mechanisms in general: by embarking on different permutations in the addition sequence of the different reagents and characterising the intermediates and products formed, this pathway can be meticulously followed from start to finish. Thus, a spectroscopic elucidation of this mechanism, supported by our previous computational studies, will extensively probe the complex yet orderly nature of this reaction, while serving as an excellent background for the study of similar multi-component reactions.

2. Experimental

2.1 Materials

All reactions involving air and moisture sensitive compounds were performed using a drybox or standard Schlenk techniques. In addition, reactions were performed using oven-dried glassware and NMR tubes. The concentration of organic solutions was carried out via a Buchi rotary evaporator connected to a tap for vacuum control. High-boiling solvents such as toluene were removed via a vacuum manifold, at a reduced pressure of 250-500 μTorr. Water soluble solvents such as 2-methoxyethanol were removed aqueous during extractions.

2-methoxyethanol in toluene (20% wt), 1,3-butadiene, copper (I) chloride, acetyl chloride, diiodomethane, and 4-ethynylbiphenyl were purchased from Sigma-Aldrich, while NBS was purified via methods reported by Dauben and McCoy.[50] CO was purchased from Praxair while 20-mesh granular zinc was previously purchased from Fisher. A day before VCP synthesis, the zinc granules were purified according to methods reported by Smith and Simmons.[51] Bottles of deuterated toluene were purchased from Cambridge laboratories, dried using sodium metal and degassed, or used without drying and degassing when acquired in ampules. Solvents were obtained from a MBRAUN solvent purification system except in the synthesis of VCP, where diethyl ether was used as purchased from Fisher Chemical. ^{1}H and ^{13}C NMR spectra were recorded via a Bruker Avance300 (^{1}H, 300 MHz, ^{13}C, 75 MHz) spectrometer. ^{1}H-NMR data were reported as follows: chemical shift (ppm), multiplicity (s = singlet, d = doublet, t = triplet, m = multiplet), coupling constant (*J*, Hz) and integration. ^{13}C-NMR data were reported as the chemical shifts of the signals.

2.2 Methods

2.2.1 Synthesis of VCP

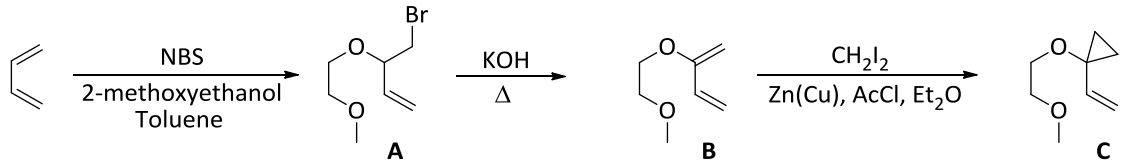

Scheme 2.1: Synthesis of 1-(2-methoxyethoxy)-1-vinylcyclopropane.[52]

The multistep sequence depicted in Scheme 2.1 was employed in the synthesis of VCP.[52] In a representative procedure, re-crystallised NBS (49.17 g, 0.28 mol) was added to 2-methoxyethanol (276.20 ml, 3.50 mol) in a 1L round-bottom flask. The flask was then cooled to -78°C via a dry ice-acetone bath. Subsequently, 124 ml of 20% wt. 1,3-butadiene in toluene solution (20 g, 0.37 mol of 1,3-butadiene) was added and the mixture was stirred for 16 hours. Afterwards, the organic solution was extracted with ether (3 x 150 ml) and then washed with brine until no more solids crashed out of solution. The organic layer was concentrated *in vacuo* and subsequently evacuated at room temperature (250-500 μTorr) to remove toluene and afford the yellow brominated intermediate **A**. While under vacuum, the solution was stirred to prevent bumping due to solvent evaporation. A vacuum was maintained for ca. 6 hours or until flask cooling from solvent evaporation had ceased.

All of compound **A** was placed in a 250 ml round-bottom flask and crushed KOH solid (40 g, 0.71 mol) was added. Subsequently, 50 ml of 2-methoxyethanol and ca. 2 ml of deionised water were added to the mixture. The flask was fitted with a condenser and heated to 72 °C for ca. 3 hours or until complete consumption of **A** was determined by TLC. While heating, the solution progressively changed colour from yellow to dark brown. Afterwards, the solution was allowed to cool to room temperature and the organic layer was extracted with pentane (3 x 150 ml). The organic solution was washed

with 150 ml of brine, dried over $MgSO_4$ and filtered to obtain a yellow solution. Pentane was subsequently distilled at ca. 60°C. The resulting solution was further concentrated at low pressure via a rotary evaporator at minimal tap-controlled pressure. Afterwards, the compound was isolated by vacuum distillation (see section 2.2.2) to afford 2.0011 g (4.2 % yield) of diene **B**.

In a 50 ml two-neck flask fitted with a condenser, purified zinc (1.7065 g, 0.0261 mol) and copper (I) chloride (0.2603 g, 0.0026 mol) were suspended in 5 ml of ether. Subsequently, diiodomethane (0.5257 ml, 0.0065 mol) followed by acetyl chloride (41.49 µL, 0.00058 mmol) were added to the flask. The mixture was heated to 45-50°C for 15 minutes until the green-gray suspension turned dark gray. Diene **B (**0.8364 g, 0.0065 mol) was added dropwise over 10 minutes after which the reaction was monitored by TLC (20% EtOAc, 80% hexanes followed by iodine staining). As the reaction progressed, a colour change from dark grey to orange was observed. The reaction was complete 30 minutes after the addition of the last drop of diene **B**. The flask was allowed to cool to room temperature and the solution was decanted into a 150 ml Erlenmeyer flask. The solids in the reaction flask were rinsed with ether (3 x 10 ml) and decanted into the Erlenmeyer flask. The resulting solution was cooled to 0°C via an ice bath and saturated NH_4Cl (20ml) was added. Afterwards, the solution was extracted with pentane (3 x 30 ml) and the resulting organic solution was washed with 1 M NaOH (3 X 30 ml) followed by brine. The organic solution was dried over $MgSO_4$, concentrated *in vacuo* under minimal pressure and vacuum distilled (see Section 2.2.2) to afford 0.3143 g (33.9% yield) of VCP **C**.

2.2.2 Purification method

Copper wire was passed through the outlet opening of a cold trap, and wound around the outer surface of the inlet tube. This tube was inserted into a pre-weighed vial and secured using the free end of the copper wire. Copper wire rings were inserted into the receiving tube in order to maximise the heat conducting properties of the trap and ensure contact between the trap and the vial. Subsequently, the secured inlet tube and vial were inserted into the receiving tube of the trap and sealed with grease. The inlet opening of the trap was connected via vacuum resistant tubing to another vial containing a stir bar and the crude diene **B** or VCP **C** (Figure 2.1). The outlet opening of the trap was connected to second trap immersed in liquid nitrogen. The second trap was then connected to the vacuum line of an Edwards pump (Figure 2.1). Both traps were evacuated at 250-500 µTorr for ca. 20 minutes.

Figure 2.1: Distillation system for product purification prior to heat application.

Afterwards, the vial was opened to vacuum for about 2 minutes while stirring the contents. The first trap (directly connected to the vial) was immersed in liquid nitrogen and the vial was heated (65-70 ˚C for **B** and 50-60 ˚C for **C**) while stirring (Figure 2.2).

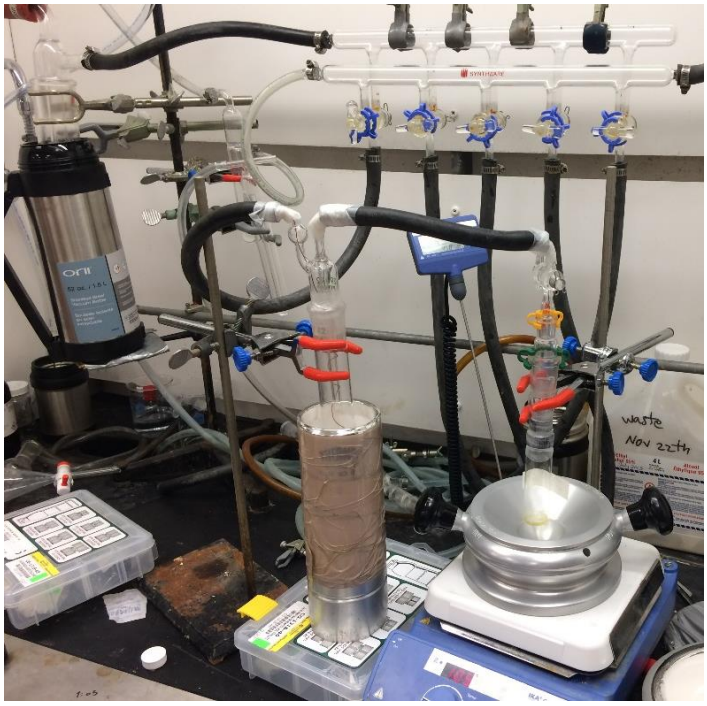

Figure 2.2: Distillation system for product purification during heating.

After boiling ceased in the vial, the system was back-filled with nitrogen gas, disassembled, and the distillate was obtained from the vial connected to the first trap. In the case of the VCP, the distillate was subsequently degassed and transferred to the drybox.

2.2.3 Spectroscopic methods

In a representative procedure where the effect of sequential catalyst and CO addition was studied, 1 eq. of VCP was reacted with 1 eq. of the catalyst and a CO pressure of 1 atm was maintained afterwards. In a drybox, a 100 MHz NMR tube was held upright in a vial and VCP (0.0070 g, 0.0492 mmol) was weighed into the NMR tube. $[RhCl(CO)_2]_2$ (0.0185 g, 0.0476 mmol) was dissolved in 0.55 ml of toluene-d_8 and the solution was transferred into the NMR tube containing the VCP, followed by thorough mixing. The tube was sealed using a rubber septum and parafilm before removal from the drybox. Subsequently, 1D and 2D ^{1}H and ^{13}C NMR experiments were run on the

sample. A thin, long stainless steel needle was used to pierce another rubber septum. The needle was removed, then attached to a CO tank via tubing and purged with the gas. Subsequently, a 21 G needle was used to pierce another hole in the septum, for venting purposes. Afterwards, the septum of the NMR tube containing the VCP + catalyst solution was quickly removed and replaced with the pierced septum. The long needle was inserted into the tube, to the bottom of the solution, while the 21 G needle was inserted for venting. CO was carefully bubbled through the solution for about 10-15 minutes. The vent needle was removed while simultaneously removing the long needle. This was done to ensure that maximum positive CO pressure was maintained in the tube. Immediately after removing both needles, the holes were sealed with grease and parafilm. Subsequently, 1D and 2D ^{1}H and ^{13}C NMR experiments were run on the resulting sample.

In a representative procedure where the effect of alkyne, catalyst and CO addition was studied, 1 equivalent of each reagent and CO (1 atm) were reacted. VCP (0.0051 g, 0.0359 mmol) was weighed into an NMR tube as described above. $[RhCl(CO)_2]_2$ (0.0143 g, 0.0368 mmol) and 4-ethynylbiphenyl (0.0062 g, 0.0348 mmol) were weighed into separate vials and subsequently combined using 0.65 ml of toluene-d_8. The resulting solution was transferred into the NMR tube containing the VCP, followed by proper mixing. The tube was sealed using a rubber septum and parafilm before removal from the drybox. Subsequently, 1D and 2D ^{1}H and ^{13}C NMR experiments were run on the sample. Afterwards, CO was introduced into the sample as described above, followed by 1D and 2D ^{1}H and ^{13}C NMR experiments.

Variable temperature reactions were carried out by heating the appropriate samples (as discussed in Section 3) in an oil bath. In addition, other catalyst concentrations as well

as different alkynes (phenylacetylene and 2-butyne) were employed according to the procedures outlined above.

2.3 NMR spectroscopic data

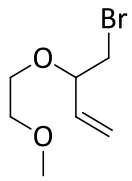

brominated intermediate A

^{1}H NMR (300 MHz, $CDCl_3$) δ 5.74 (ddd, *J* = 17.24, 10.26, 7.13 Hz, 1H), 5.29-5.38 (m, 2H), 3.97 (q, *J* = 5.83 Hz, 1H), 3.74-3.66 (m, 1H), 3.62-3.52 (m, 3H), 3.46-3.33 (m, 5H).

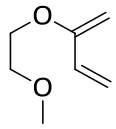

diene B

^{1}H NMR (300 MHz, $CDCl_3$) δ 6.16 (dd, *J* = 17.23, 10.78 Hz, 1H), 5.62 (dd, *J* = 17.23, 1.68 Hz, 1H), 5.11 (d, *J* = 10.79 Hz, 1H), 4.15 (s, 2H), 3.93-3.90 (m, 2H), 3.72-3.70 (m, 2H), 3.43 (s, 3H). ^{13}C NMR (75 MHz, $CDCl_3$) δ 158.20, 133.03, 114.38, 87.09, 70.80, 66.76, 59.03.

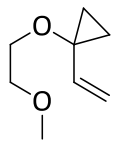

VCP C

^{1}H NMR (300 MHz, $CDCl_3$) δ 5.64 (dd, *J* = 17.28, 10.70 Hz, 1H), 5.21 (dd, *J* = 17.28, 1.50 Hz, 1H), 5.07 (dd, *J* = 10.70, 1.50 Hz, 1H), 3.64-3.61 (m, 2H), 3.53-3.49 (m, 2H), 3.38 (s, 3H), 1.08-1.04 (m, 2H), 0.73-0.69 (m, 2H). ^{13}C NMR (75 MHz, $CDCl_3$) δ 138.91, 112.20, 71.98, 66.92, 61.86, 59.03, 14.53.

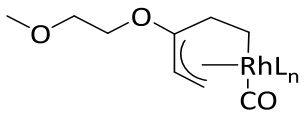

INT B

^{1}H NMR (300 MHz, toluene-d$_8$) δ 4.64 (ddd, *J* = 10.63, 4.54, 2.93 Hz 1H), 4.50 (dd, *J* = 10.84, 8.33 Hz, 1H), 3.86-3.79 (m, 1H), 3.61-3.54 (m, 1H), 3.38-3.32 (m, 1H), 3.30-3.19 (m, 1H), 3.15 (s, 3H), 2.89-2.84 (m, 1H), 2.16 (dd, *J* = 4.44, 2.37 Hz, 1H) 1.92-1.84 (m, 1H), 1.31-1.24 (m, 1H), 1.11 (ddd, *J* = 10.48, 4.19, 2.91 Hz, 1H). ^{13}C NMR (toluene-*d*$_8$) δ 81.39, 70.07, 69.48, 58.28, 51.85, 29.44, 29.22, 26.43.

3. Results and Discussion

3.1 Computational investigation on the [5 + 1 + 2 + 1] cycloaddition reaction

Prior to the spectroscopic investigation reported in this thesis, a thorough computational study[53] was performed at the ωB97XD[45]/def2TZVPP[46] level of theory as shown in Figure 3.1. Our calculations revealed two competing cycloaddition pathways: the [5 + 1 + 2 + 1] (blue) and the [5 + 1 + 1 + 2] (black) pathways. In addition, we showed that off-metal cyclization and aromatization (red) is higher energy than the on-metal pathway.

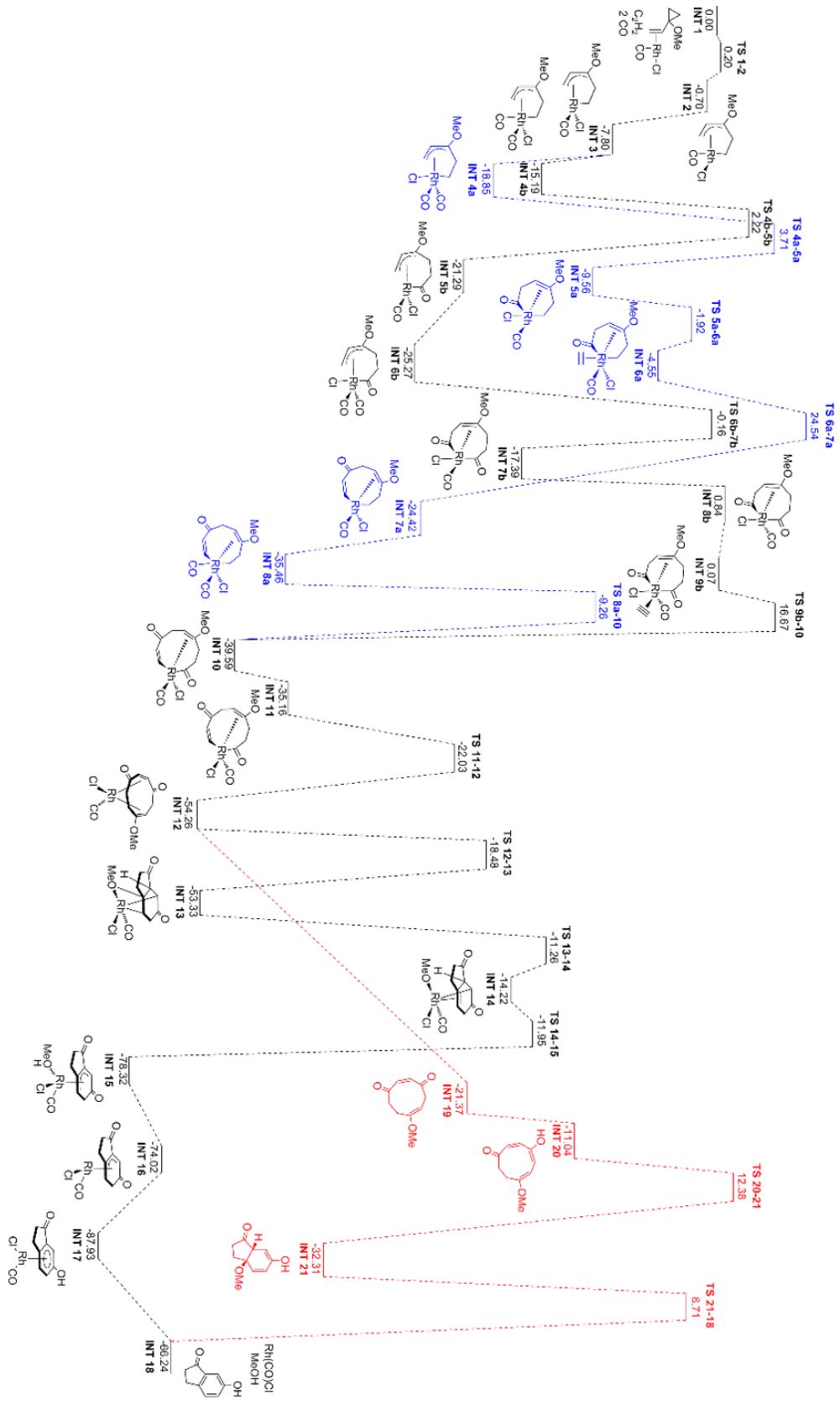

Figure 3.1: Potential energy surface (kcal/mol) of the Rh-catalysed [5 + 1 + 2 + 1] cycloaddition.[53]

The existence of high alkyne-insertion barriers in both cycloaddition pathways (>40kcal/mol) as well as the high off-metal cyclization and aromatization pathway elicited the spectroscopic investigation reported herein. To begin this investigation, VCP was synthesised (Sections 2.2.1 and 2.2.2) [52] and characterised as reported in section 3.2.

3.2 Modifications to synthetic methods reported by Wender

The methods reported in Section 2 were adapted from that reported by Wender.[52] However, these methods reported herein were designed to accommodate the available materials. For instance, 1,3-butadiene with toluene as the carrier solvent was used in the synthesis of diene **B**, instead of condensed 1,3-butadiene as reported by Wender. The inability to purchase gaseous 1,3-butadiene was the reason for the choice of the 1,3-butadiene - toluene solution.

After bromination of 1,3-butadiene, the one-pot elimination procedure reported by Wender was attempted. However, the failure to obtain diene **B** elicited the need for a new route. While Wender reported the addition of KOH to intermediate **A** at room temperature, the isolation of this intermediate and the subsequent elimination reaction at 72 ˚C afforded diene **B**. It is possible that previous attempts to synthesise diene **B** by the one-pot elimination method failed as a result of insufficient heat. Since Wender performed this elimination reaction on a large scale, the heat generated upon the addition of KOH at room temperature[52] may have facilitated the formation of diene **B**. For this project, the elimination reaction was performed on a small scale. Hence, a room temperature approach generated insufficient heat and the need for an external heat source was critical. In addition, when the one-pot elimination method was attempted at a higher temperature, it proved difficult to isolate diene **B**. While 2-methoxyethanol was easily removed during extraction, toluene remained in the organic phase. Although

column chromatography was attempted in the removal of toluene, diene **B** degraded in the column probably due to the acidity of the silica gel used. Thus, it was pertinent that toluene was removed by evacuation prior to the synthesis of diene **B**. The low diene **B** yield reported herein, may have resulted from the use of the 1,3-butadiene – toluene solution instead of the condensed 1,3-butadiene.

In the synthesis of VCP, the approach reported by Wender was modified. This is because when the reagents were allowed to react for a total of 5.5 hours (as reported by Wender) both VCP and a double cyclopropanation product were obtained (see Appendix, Figure 7.4). In addition, Wender reported the addition of excess diiodomethane. This, in combination with the long reaction time may have caused the double cyclopropanation that occurred in earlier, small scale trials. Thus, in later VCP syntheses, the reactions were monitored by TLC and equimolar amounts of diene **B** and diiodomethane were used.

3.3 Spectroscopic data on the synthesis of VCP

Figures 3.2, 3.3 and 3.5 shows the ^{1}H-NMR spectra of compounds **A, B** and **C** respectively, while Figures 3.4 and 3.6 show the ^{13}C-NMR spectra of compounds **B** and **C** respectively.

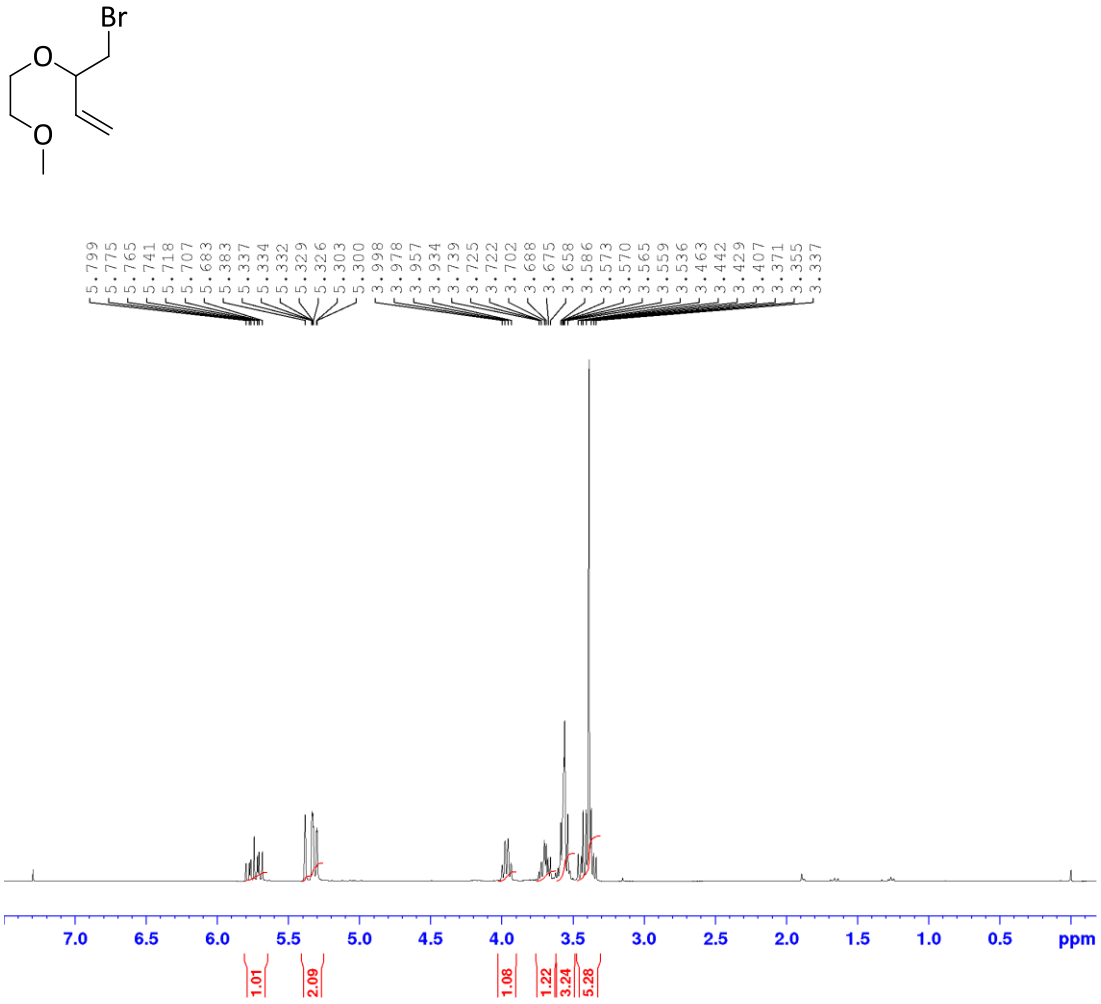

Figure 3.2: ^{1}H NMR (300 MHz, $CDCl_3$) spectrum of brominated intermediate A.

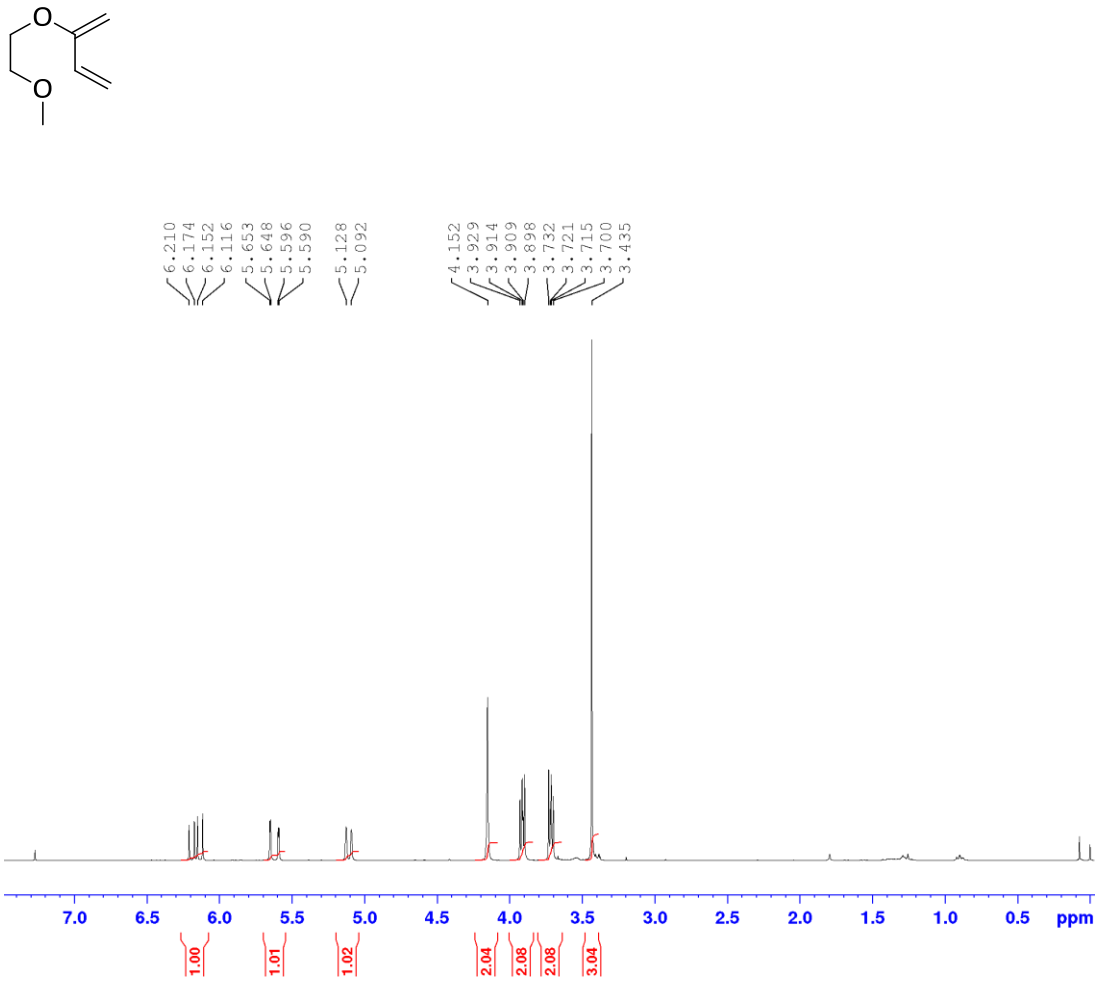

Figure 3.3: ^{1}H NMR (300 MHz, $CDCl_3$) spectrum of diene B.

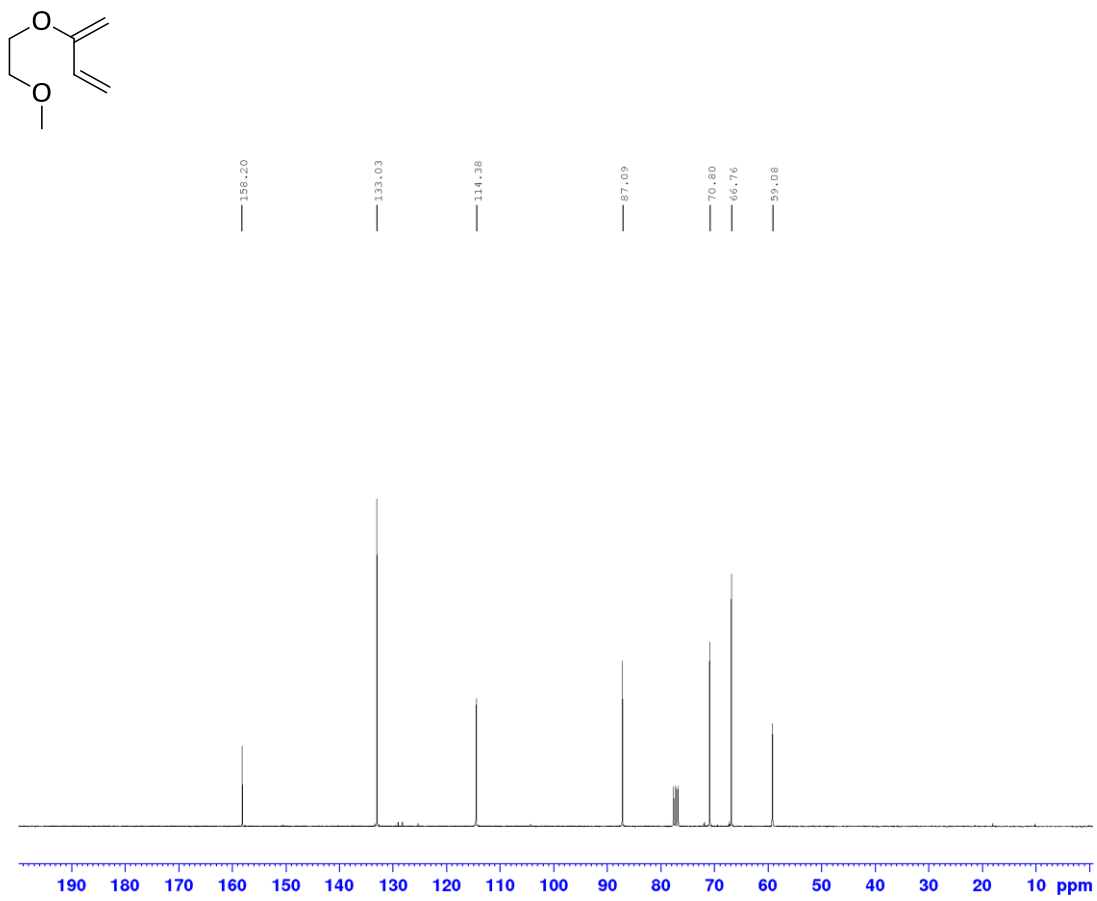

Figure 3.4: ^{13}C NMR (75 MHz, $CDCl_3$) spectrum of diene B.

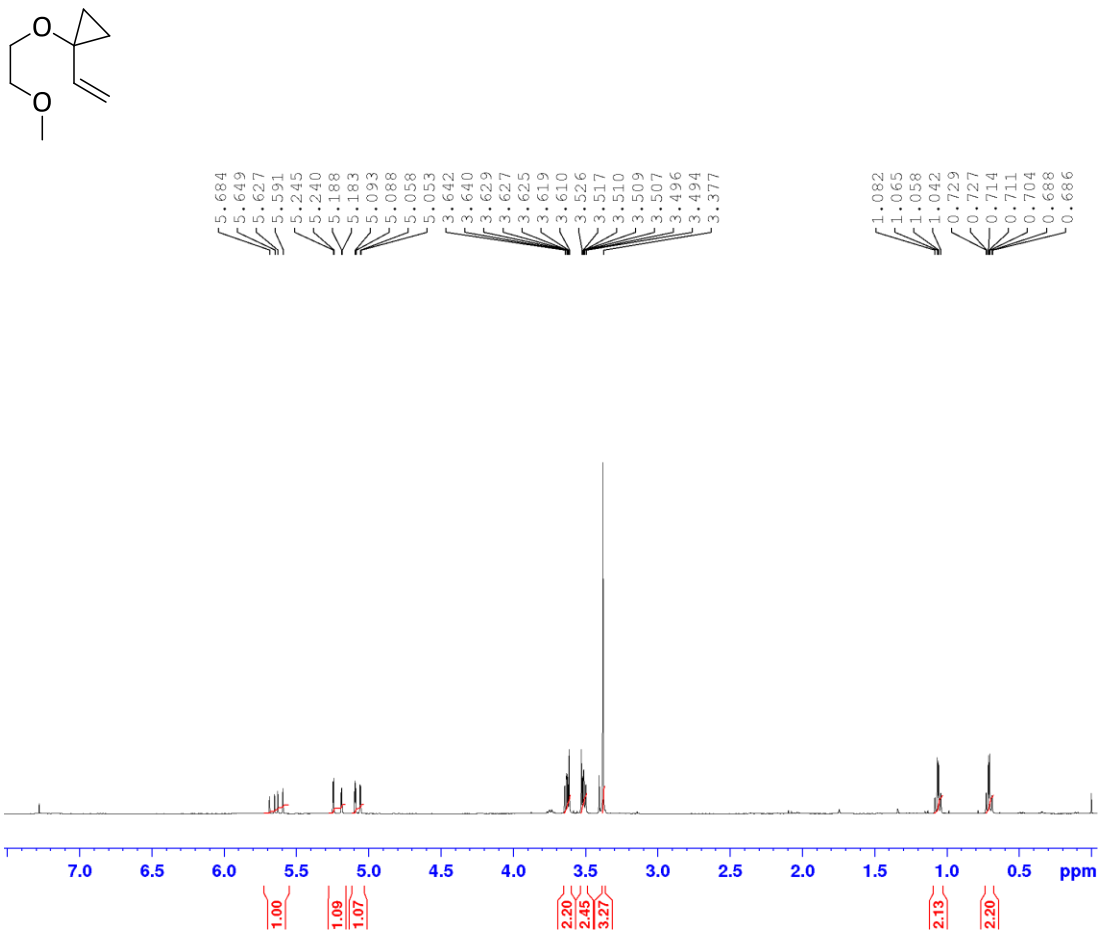

Figure 3.5: ^{1}H NMR (300 MHz, $CDCl_3$) spectrum of VCP C.

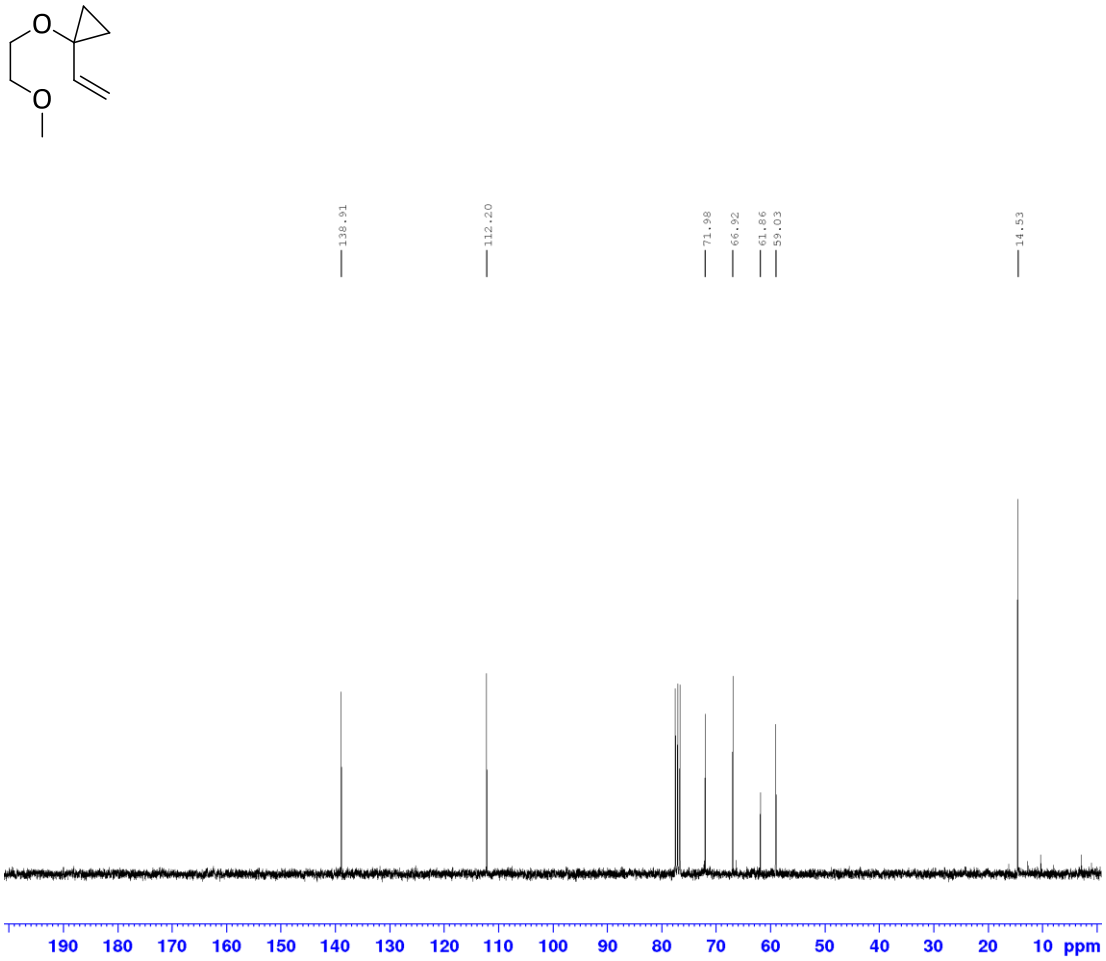

Figure 3.6: ^{13}C NMR (75 MHz, $CDCl_3$) spectrum of VCP C.

3.4: Spectroscopic data analysis on the mechanistic investigation of the [5 + 1 + 2 + 1] cycloaddition

When 1 equiv. of VCP was reacted with 1 equiv. of $[RhCl(CO)_2]_2$ under N_2, a ^1H NMR spectrum (Fig. 3.7) revealed the existence of at least two species. These species, as indicated by the two methyl peaks at 3.15 ppm and 3.13 ppm, are possibly analogues of INT 3 and INT 4a shown in Fig. 3.1. The peak at 1.0-0.7 ppm was due to H-grease while the peak at 0.3-0.2 was due to silicon grease.[54]

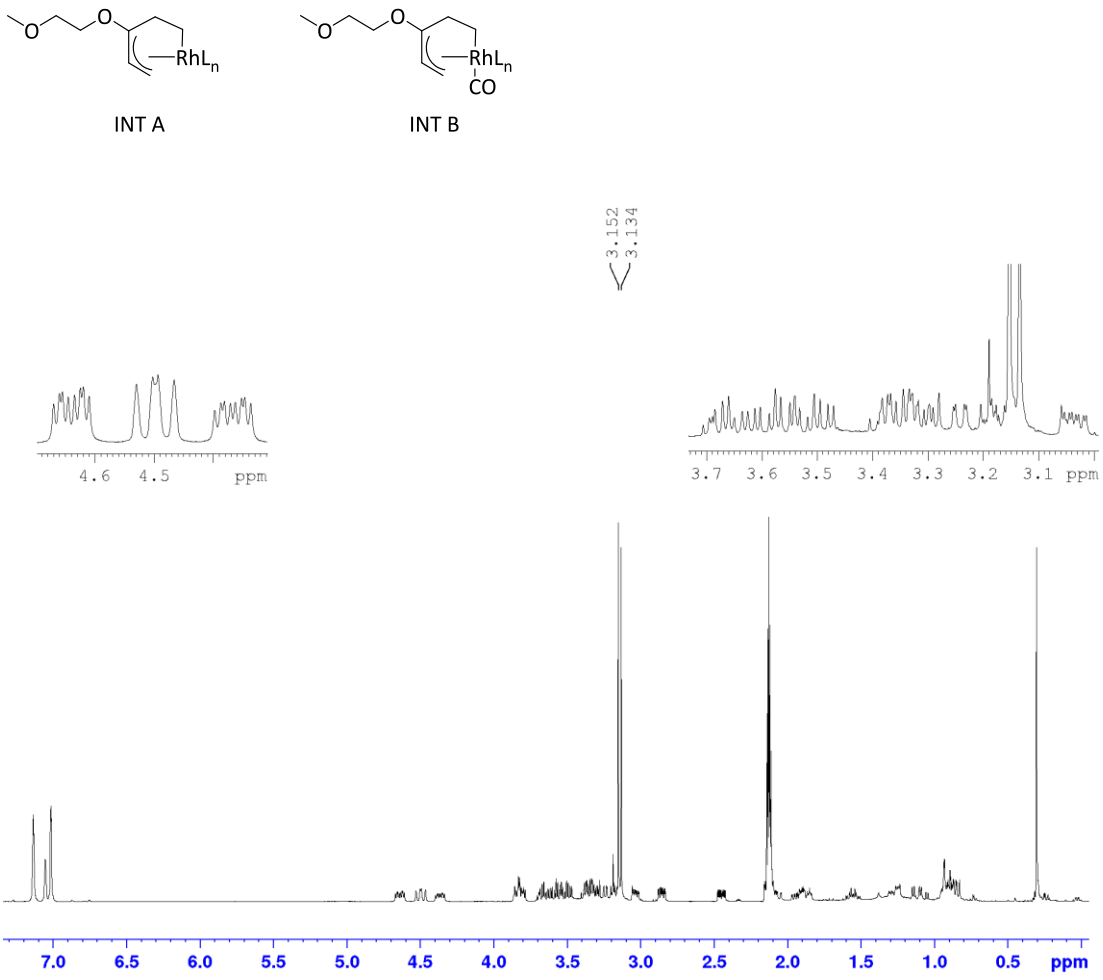

Figure 3.7: ^1H NMR (300 MHz, toluene-d_8) spectrum of VCP + Rh-catalyst.

Computational calculations showed that the methoxy substituted analogues, INT 2 and INT 3, resulted from a low energy C-C bond activation barrier of 0.2 kcal/mol. Upon

the coordination of CO, INT 4 is formed. It is pertinent to note that while INT 2 and INT 3 may have similar spectra signals and chemical shifts, INT 4 may have a different spectrum as a result of changes in its electronic nature due to CO coordination. CO displaced from the catalyst during C-C bond activation of VCP, may have coordinated to the 2-methoxyethoxy analogue of INT 3, to yield the corresponding analogue of INT 4a. This hypothesis was the rationale for the assignment of the 2-methoxyethoxy substituted species (INT A and INT B) shown in Fig. 3.7.

Upon bubbling CO through a sample of VCP and the catalyst, a ^{1}H NMR spectrum revealed the retention of only one species, as indicated by the presence of 1 methyl peak (Figure 3.8, 3.16 ppm). Thus, it was inferred that the coordination of CO to the metal centre resulted in the formation of the lower energy species. This species, INT B, is possibly the 2-methoxyethoxy analogue of INT 4a (Fig. 3.1), as INT 4a was computationally shown to result from CO coordination.

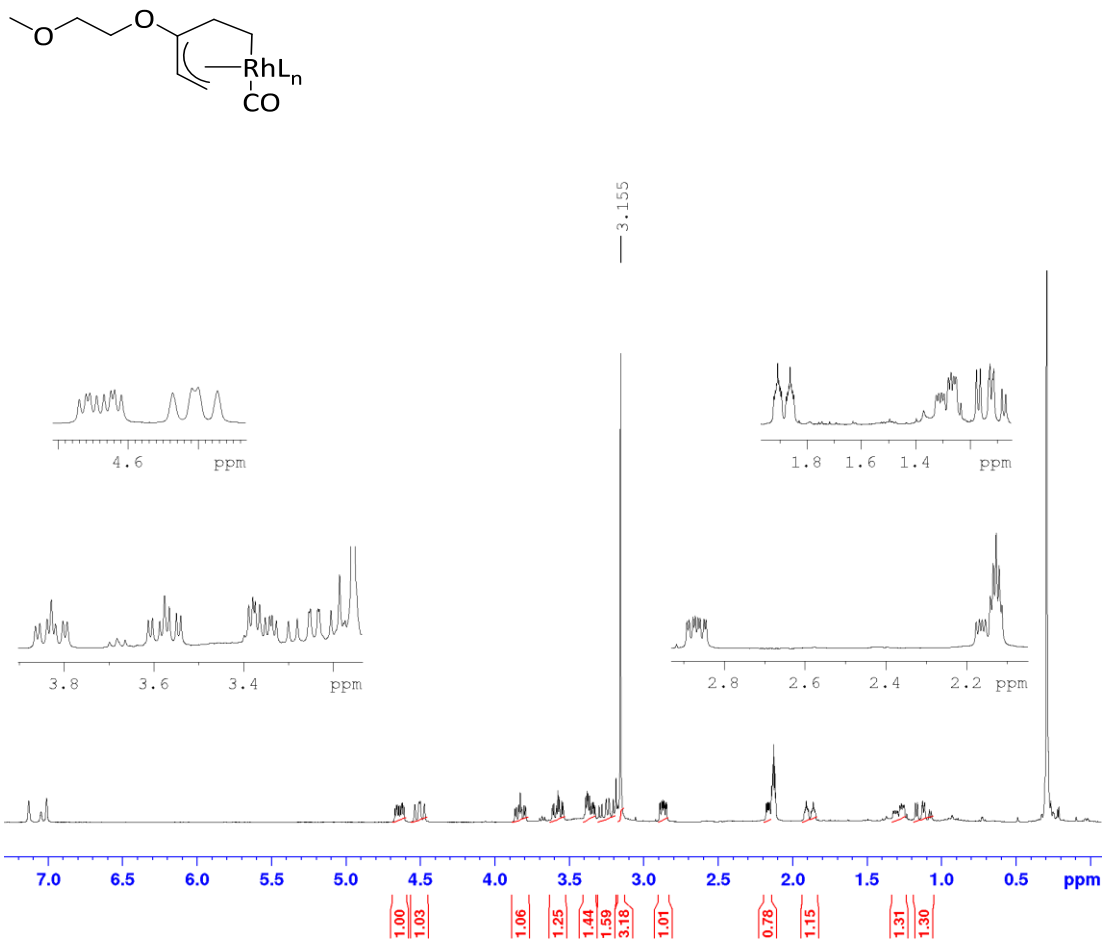

Figure 3.8: ^{1}H NMR (300 MHz, toluene-d$_8$) spectrum of INT B.

In the effort to determine the nature of INT B, a 2D-COSY experiment was performed and the resulting spectrum is shown in Figure 3.9 a-d.

a

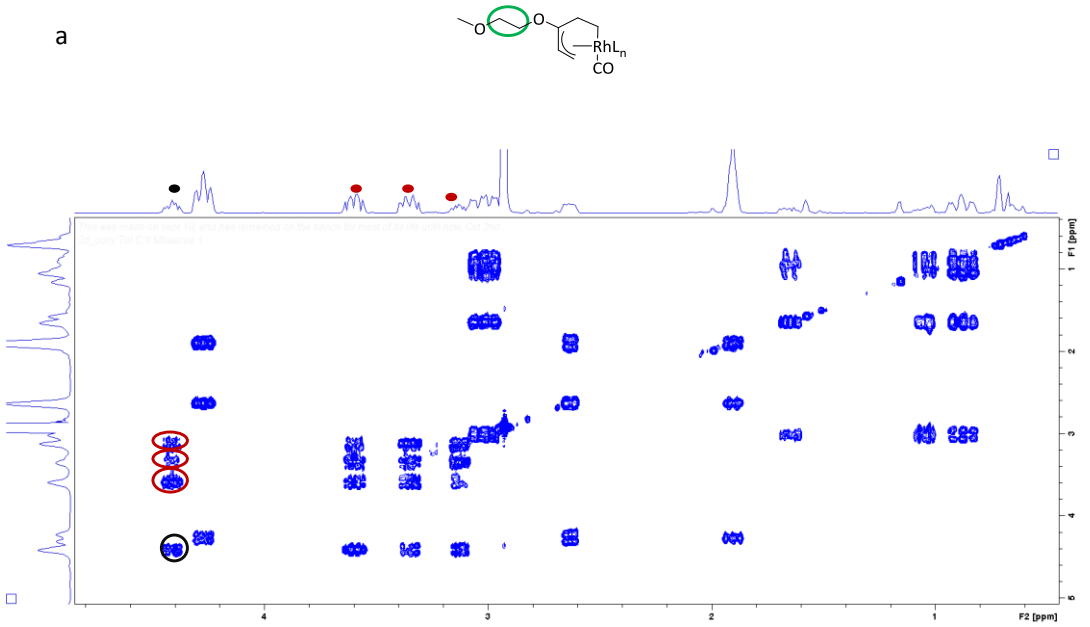

b

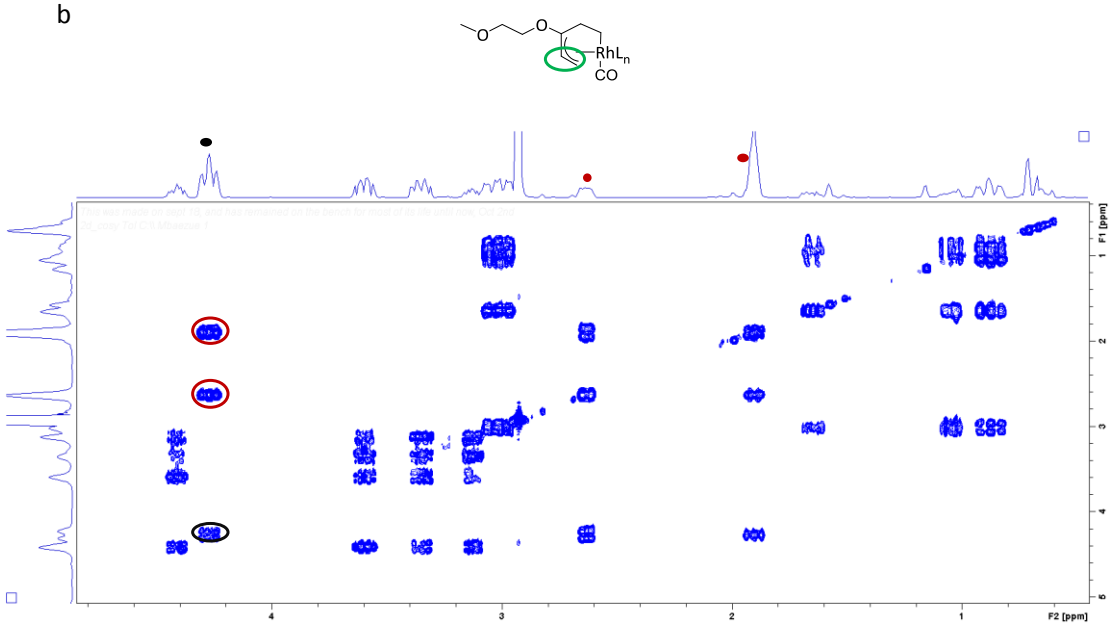

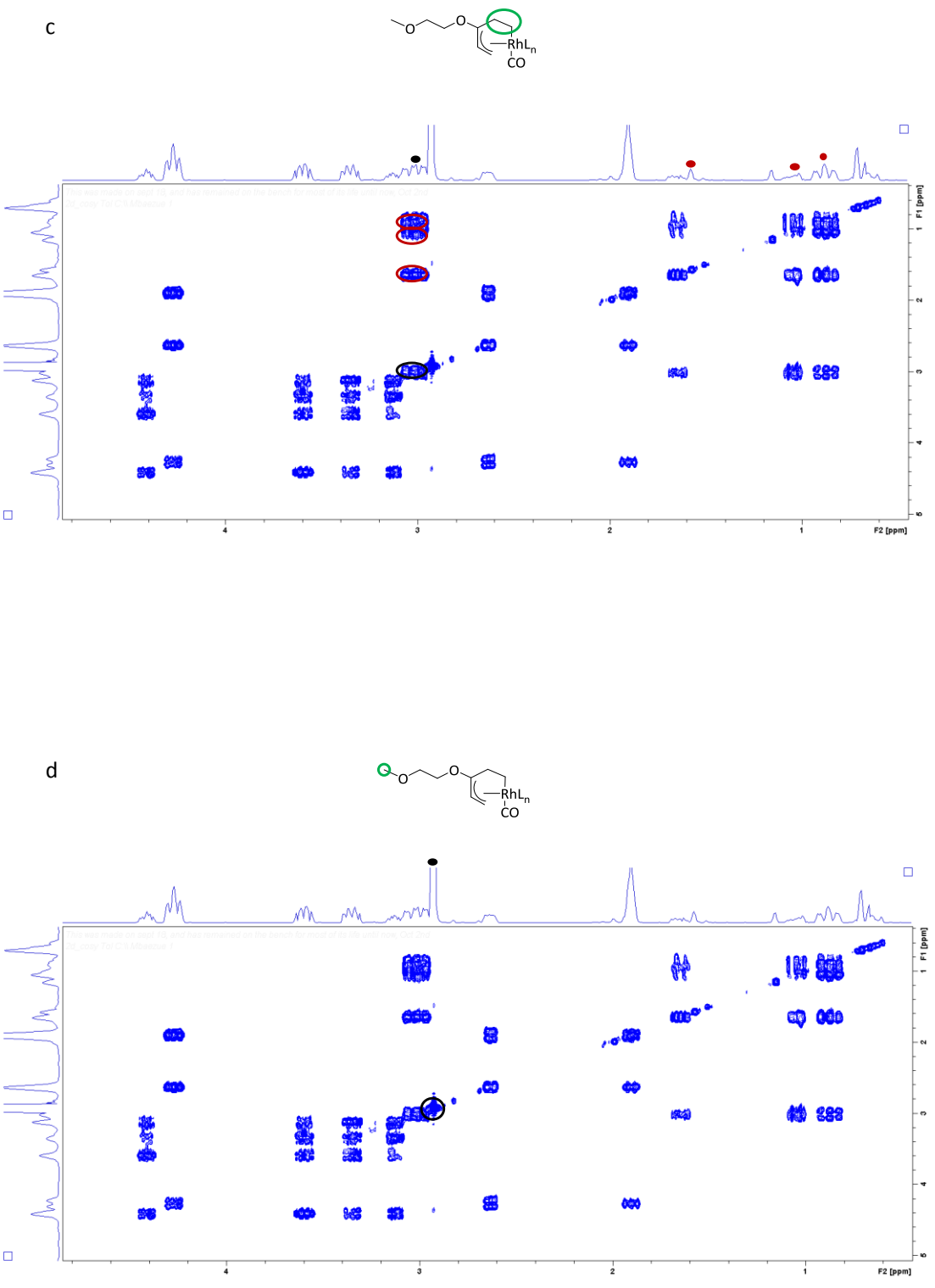

Figure 3.9 a-d: 2D COSY NMR (toluene-d_8) spectrum of INT B.

This Figure shows the ^{1}H assignments based upon the hypothesis that the CO-coordination complex is formed upon the addition of CO. While the assigned proton is indicated by a black oval on the 1D-axis and a black dot on the 2D-axis, the coupled protons are indicated as red dots on the 2D-axis. In addition, the green oval highlights the proton environments being considered. It should be noted that the peak at 2.2 ppm (Figure 3.9) overlaps with a toluene-d_8 solvent peak. However, Figure 3.8 resolves both peaks.

To further probe these assignments, a DEPT-Q experiment was run on the sample (Figure 3.10).

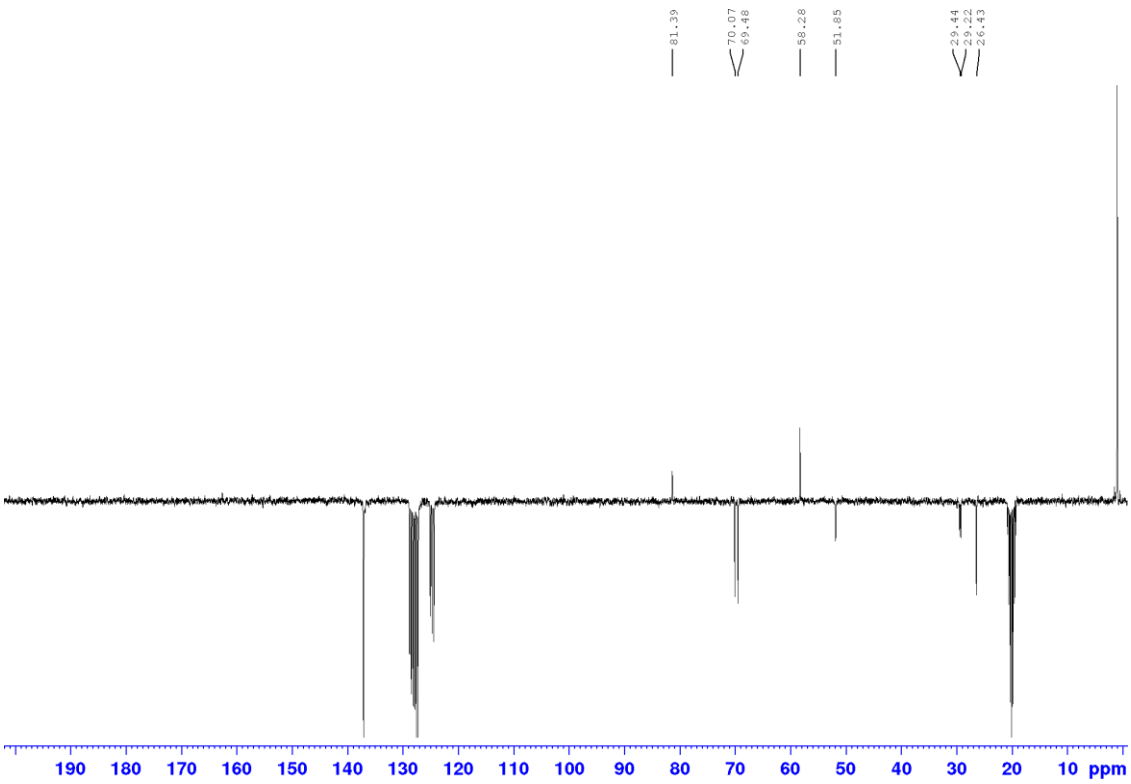

Figure 3.10: DEPT-Q (toluene-d_8) spectrum of INT B.

In Figure 3.10, both positive signals at 81.39 ppm and 51.85 ppm are indicative of the methine and methyl carbon atoms respectively, while the negative signals are indicative

of the remaining 6 carbon atoms in the carbon skeleton of the C-C bond activated moiety.

A HSQC experiment, in combination with the DEPT-Q experiment was used to further assign the proton and carbon atoms in the C-C bond activated moiety of INT B (Figure 3.11 a-p).

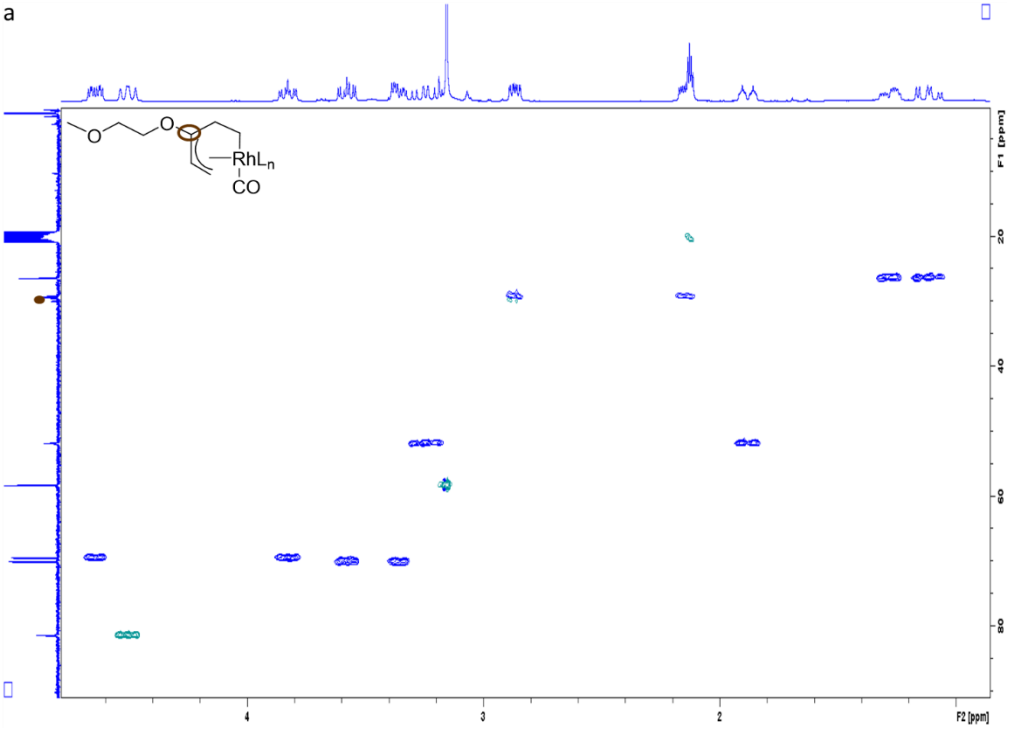

b

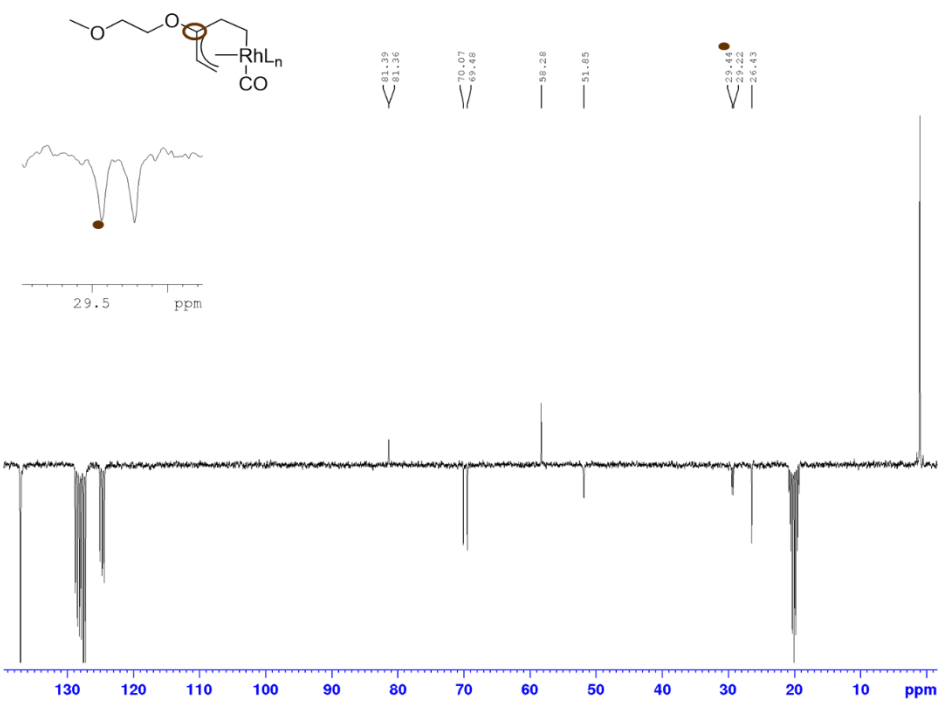
RhL$_n$
CO
81.39
81.36
70.07
69.48
58.28
51.85
29.44
29.22
26.43
29.5
ppm
130
120
110
100
90
80
70
60
50
40
30
20
10
ppm

c

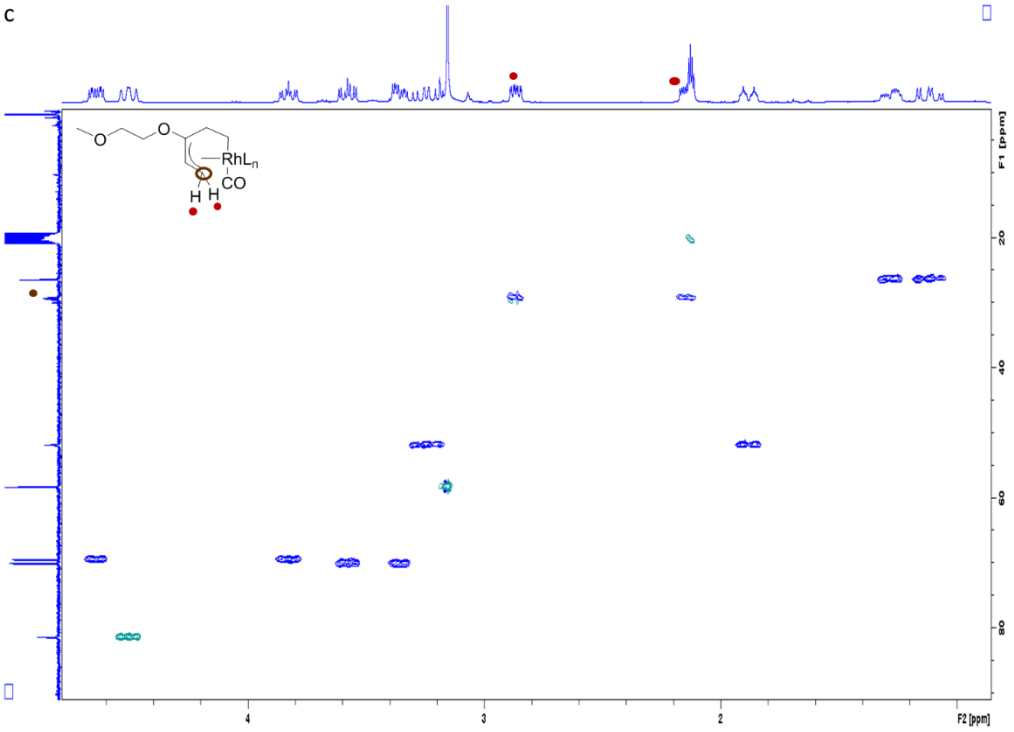
RhL$_n$
CO
H H
F1 [ppm]
20
40
60
80
4
3
2
F2 [ppm]

d

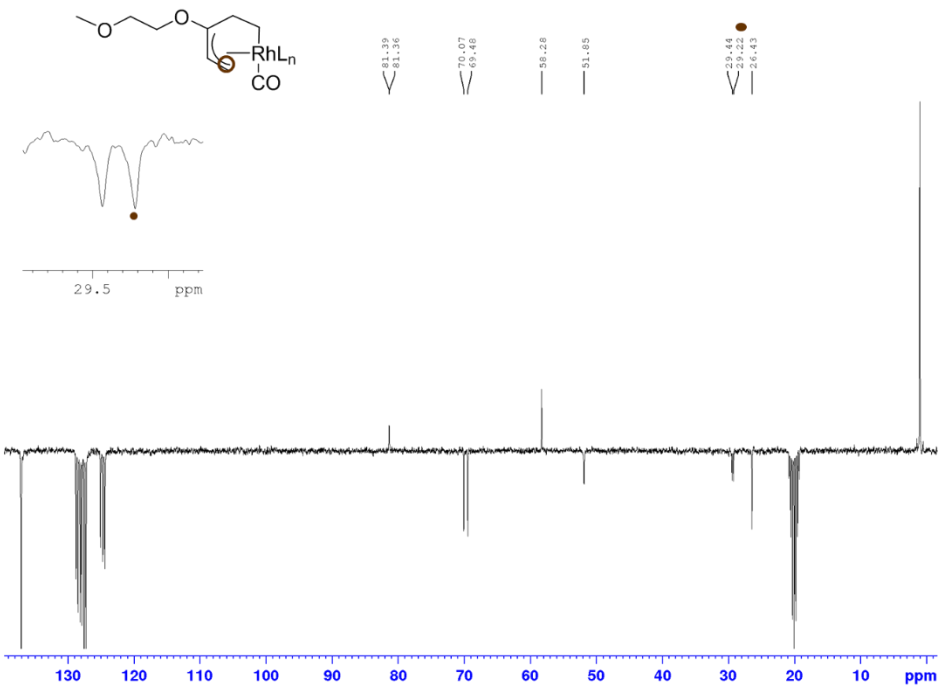
RhLn
CO
81.39
81.36
70.07
69.48
58.28
51.85
29.44
29.22
26.43
29.5
ppm
130
120
110
100
90
80
70
60
50
40
30
20
10
ppm

e

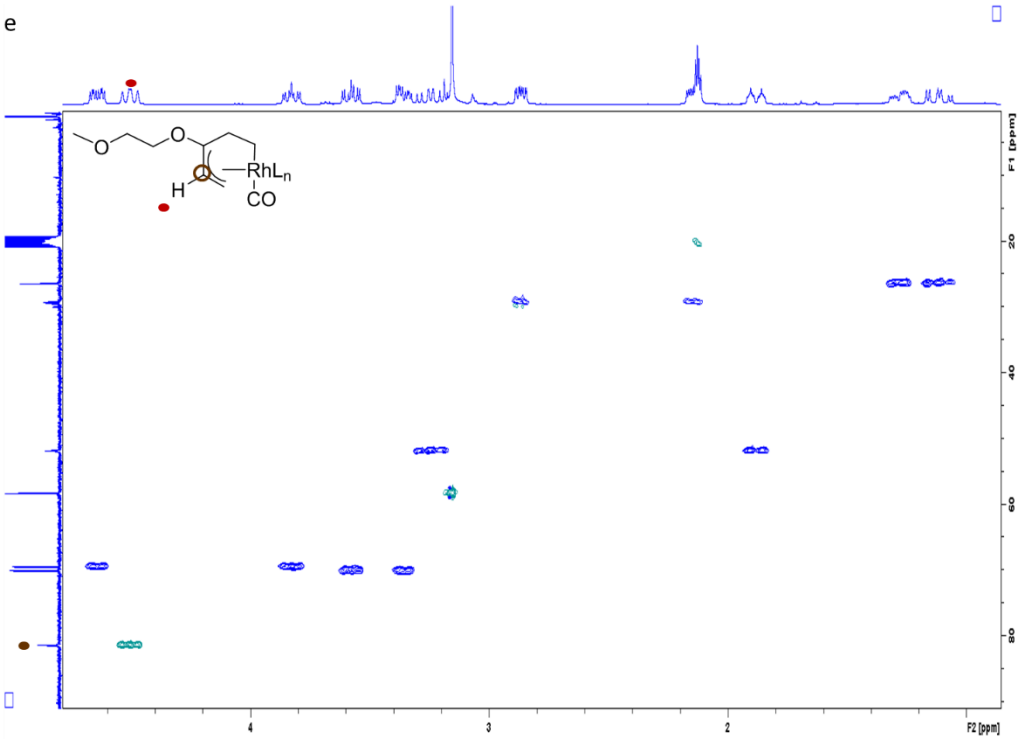
RhLn
CO
H
F1 [ppm]
20
40
60
80
4
3
2
F2 [ppm]

f

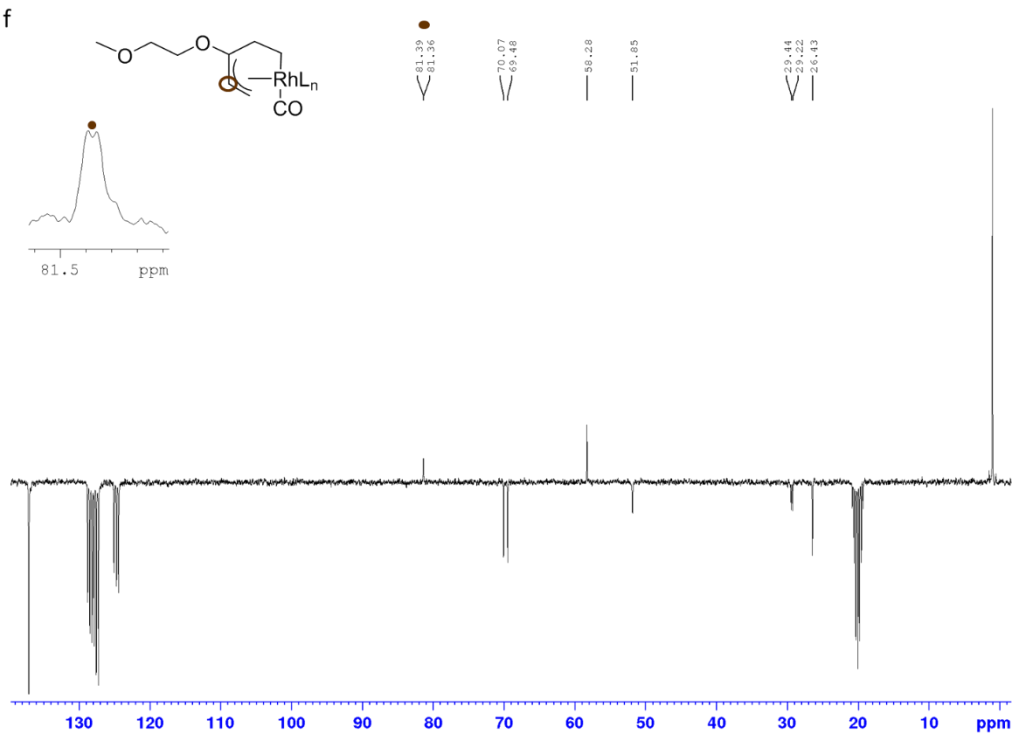
81.39
81.36
70.07
69.48
58.28
51.85
29.44
29.22
26.43
81.5
ppm
130
120
110
100
90
80
70
60
50
40
30
20
10
ppm

g

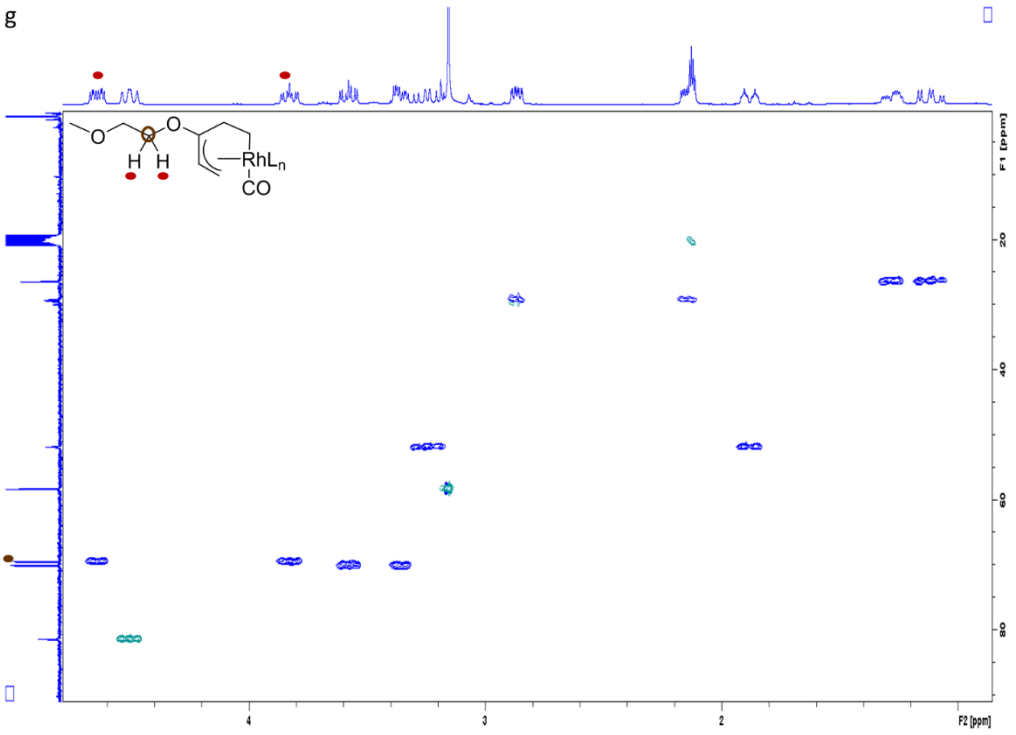
F1 [ppm]
F2 [ppm]

h

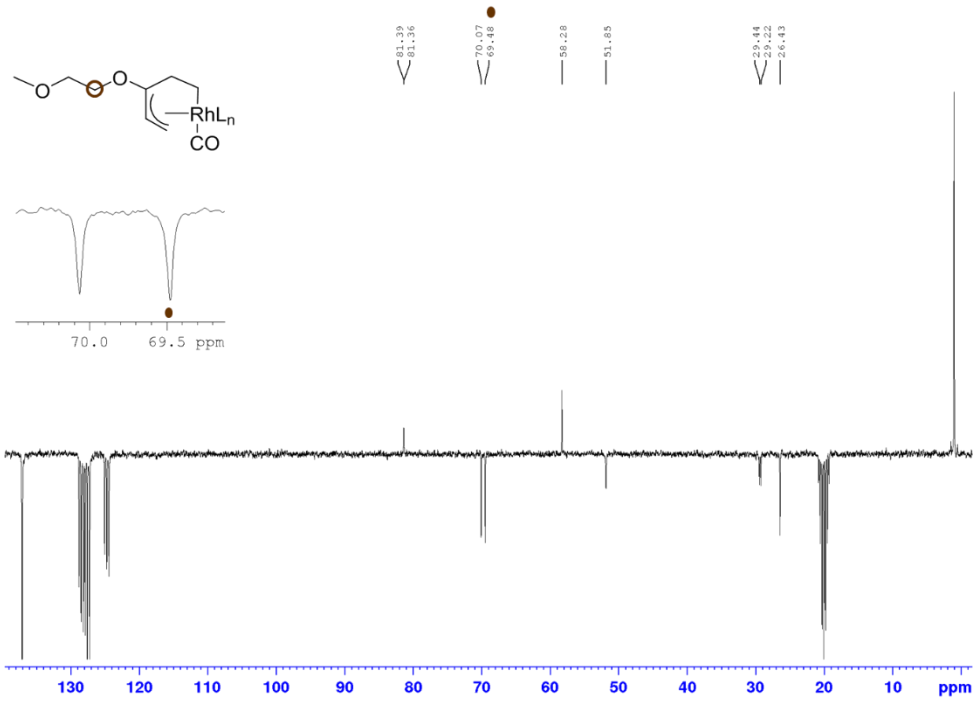
81.39
81.36
70.07
69.48
58.28
51.85
29.44
29.22
26.43
RhLn
CO
70.0
69.5 ppm
130
120
110
100
90
80
70
60
50
40
30
20
10
ppm

i

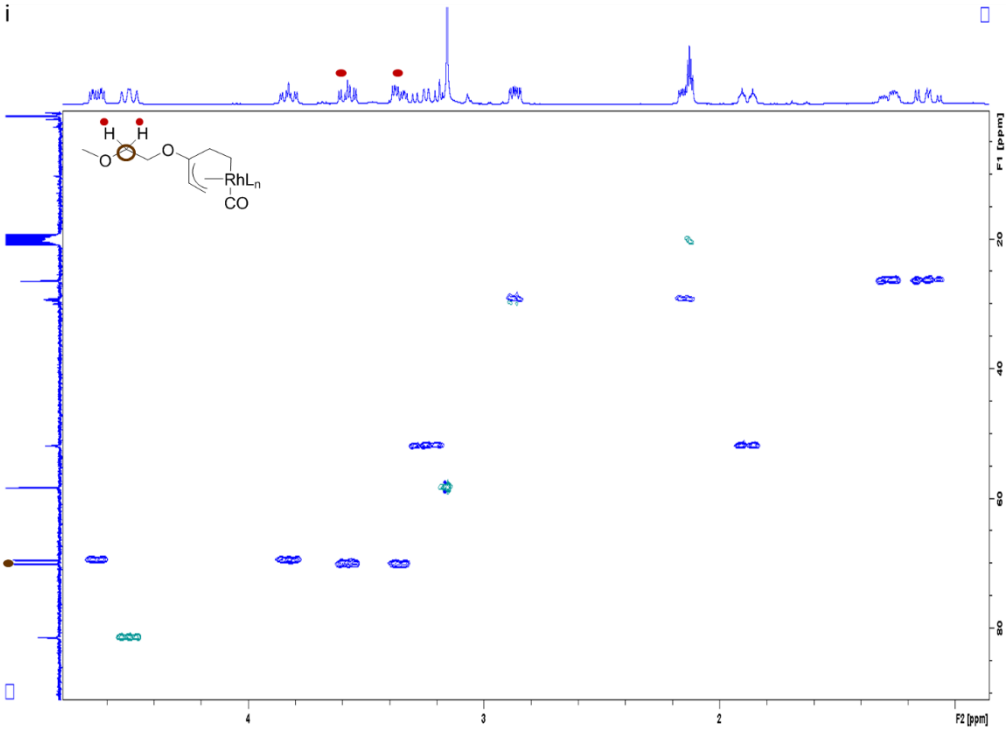
H
H
RhLn
CO
F1 [ppm]
20
40
60
80
4
3
2
F2 [ppm]

j

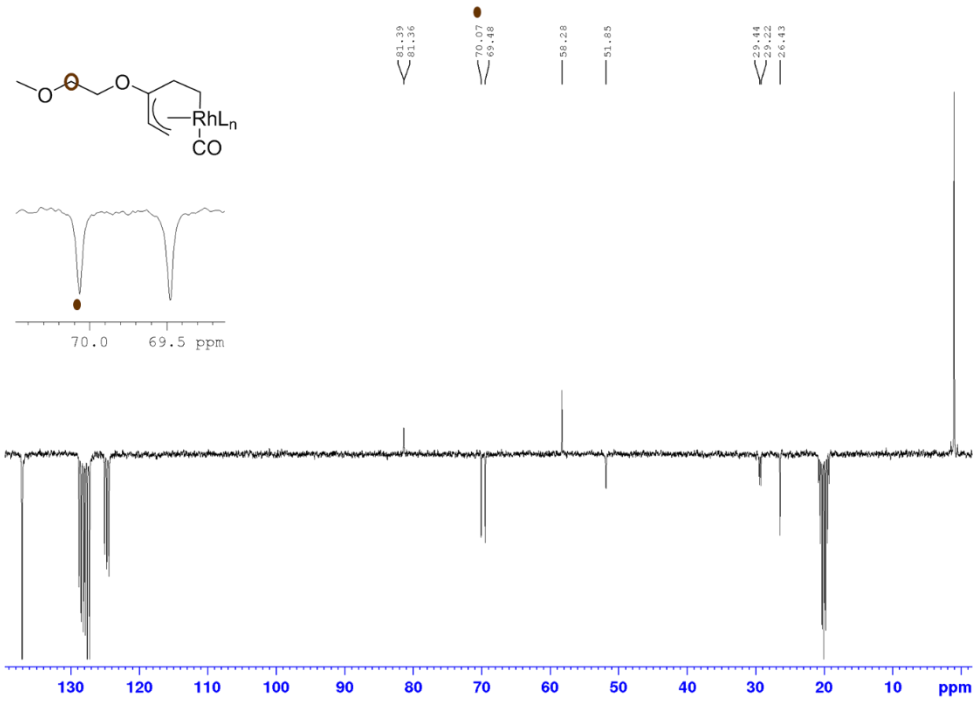
81.39
81.36
70.07
69.48
58.28
51.85
29.44
29.22
26.43
RhLn
CO
70.0
69.5 ppm
130
120
110
100
90
80
70
60
50
40
30
20
10
ppm

k

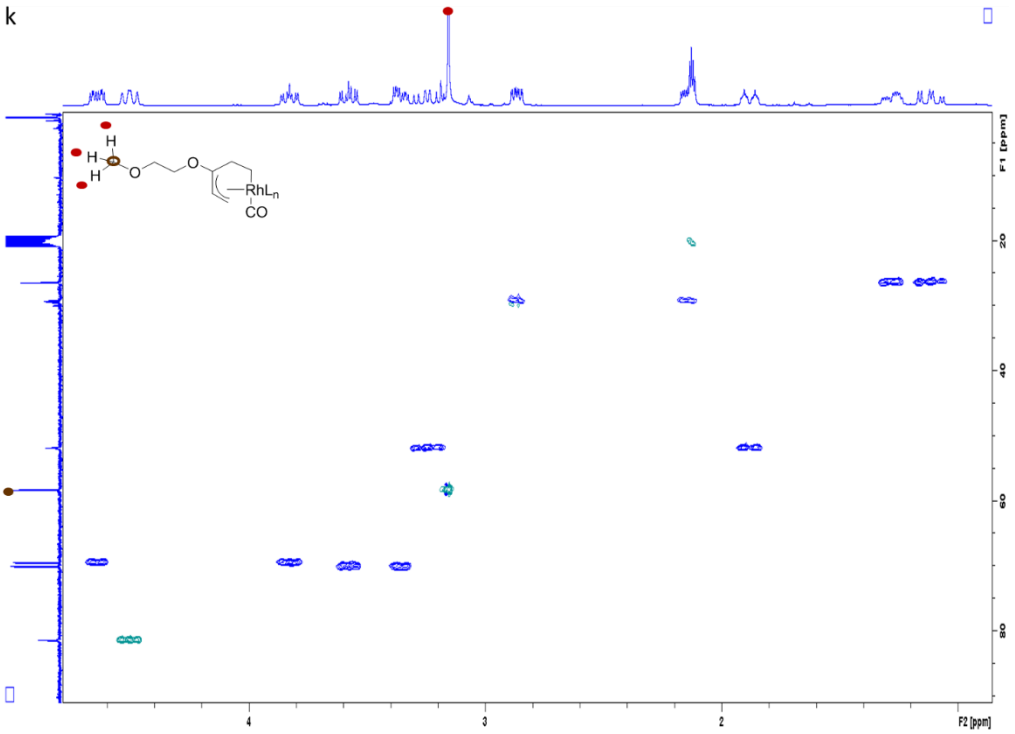
H
H
H
O
O
RhLn
CO
F1 [ppm]
20
40
60
80
4
3
2
F2 [ppm]

l

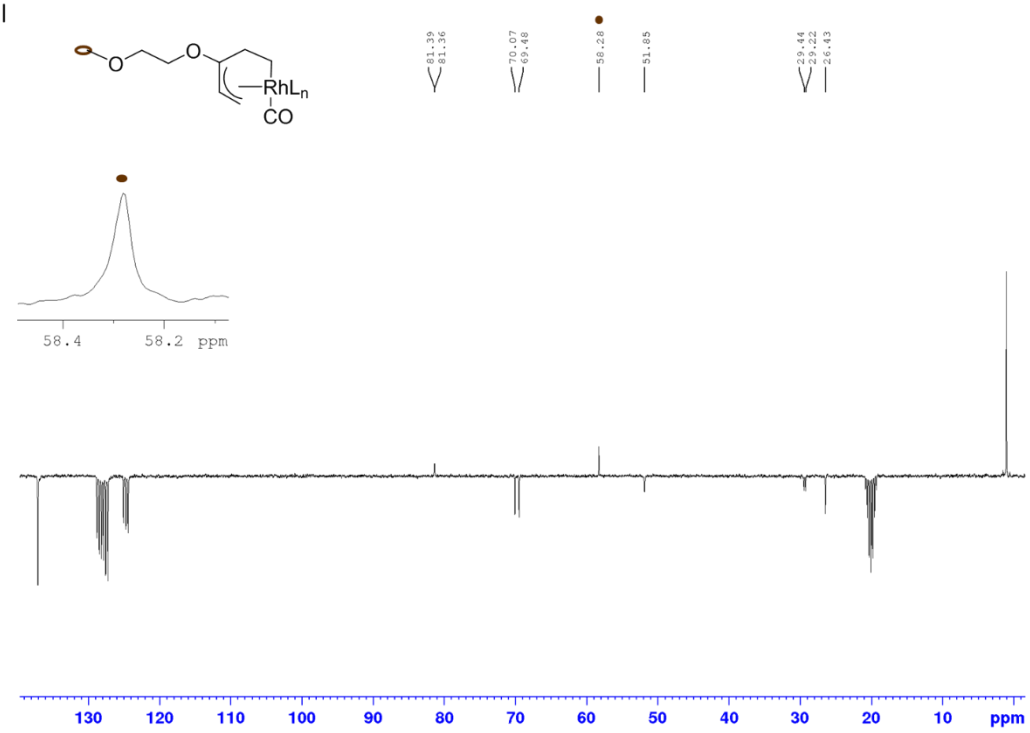
O
O
RhLn
CO
81.39
81.36
70.07
69.48
58.28
51.85
29.44
29.22
26.43
58.4
58.2 ppm
130
120
110
100
90
80
70
60
50
40
30
20
10
ppm

m

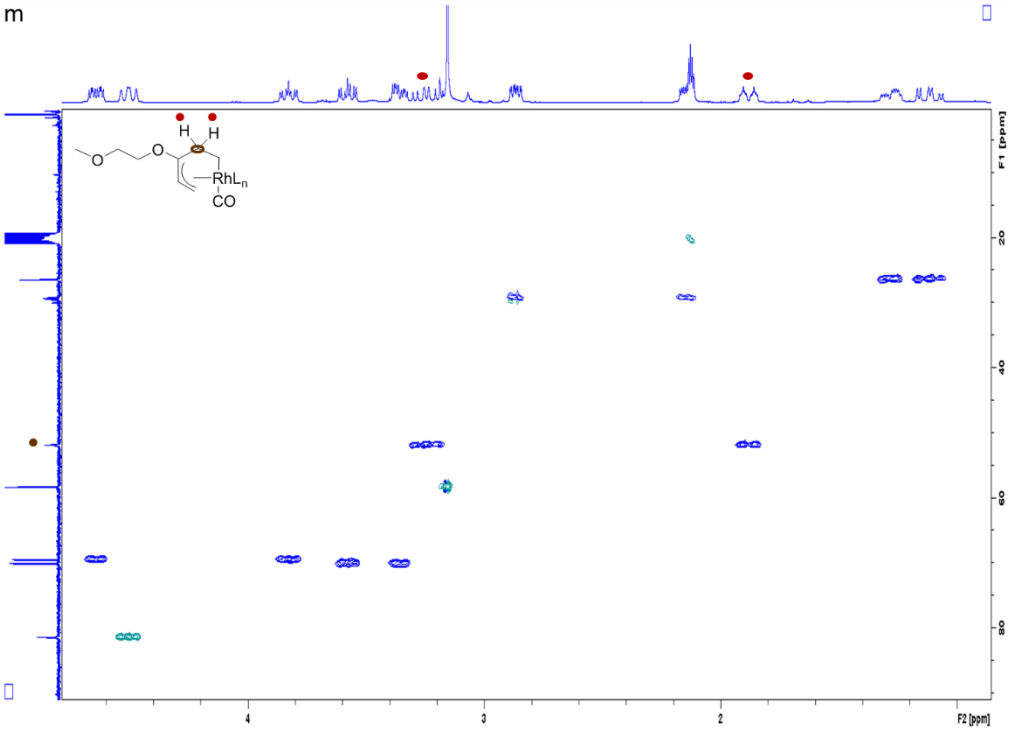
H
H
O
O
RhLn
CO
F1 [ppm]
20
40
60
80
4
3
2
F2 [ppm]

n

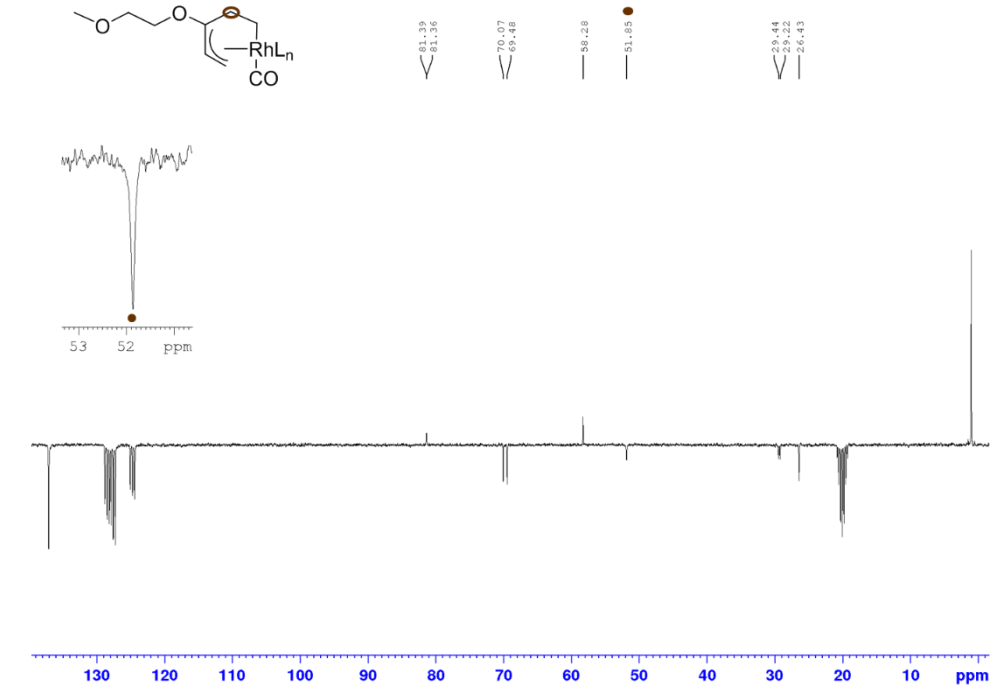
RhLn
CO
81.39
81.36
70.07
69.48
58.28
51.85
29.44
29.22
26.43
53
52
ppm
130
120
110
100
90
80
70
60
50
40
30
20
10
ppm

o

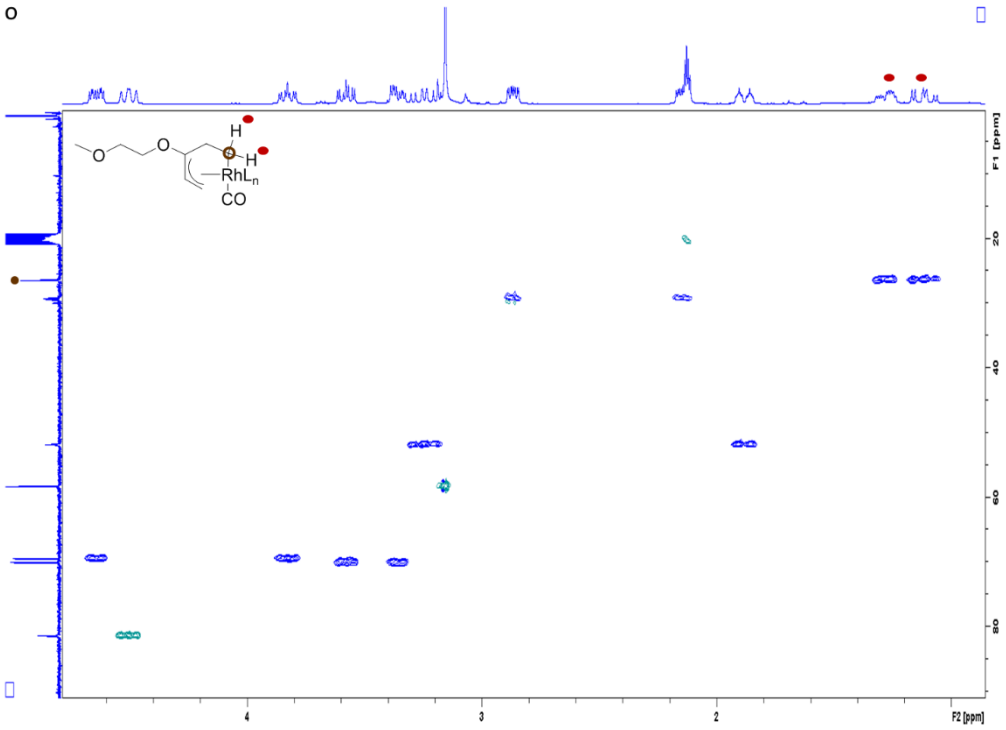
H
H
RhLn
CO
F1 [ppm]
F2 [ppm]

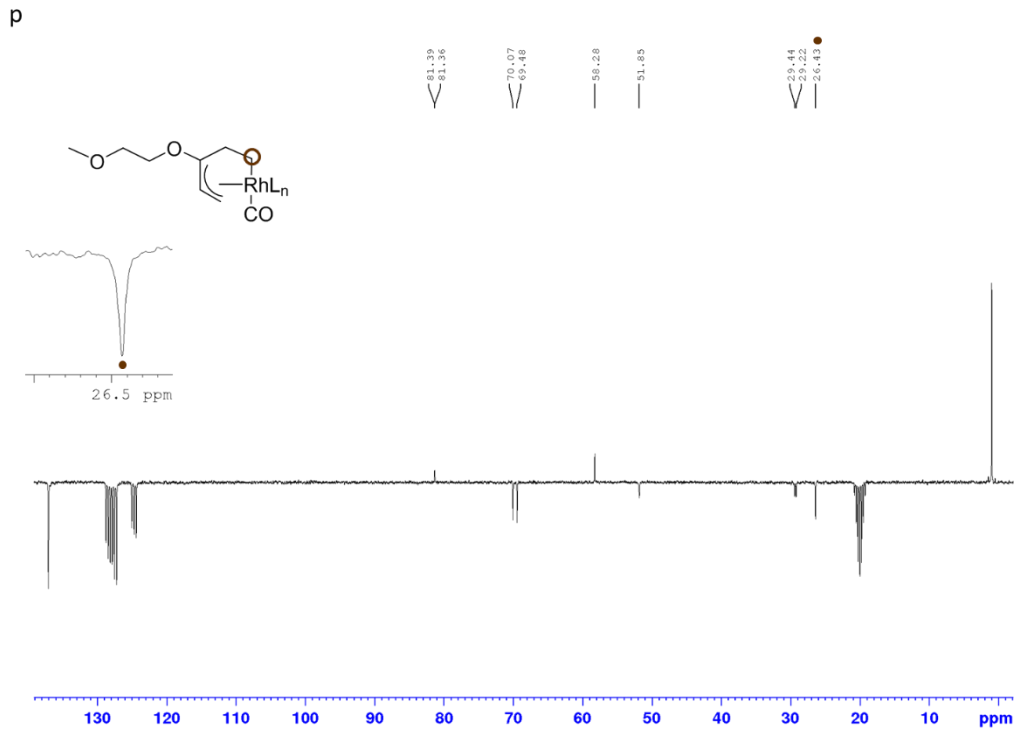

Figure 3.11 a-p: HSQC and DEPT-Q (toluene-d_8) experiments in the characterisation of INT B.

In Fig. 3.11 a-d, the brown ovals and brown dots represent the carbon atoms and the carbon signals respectively, while the red dots represent the coupled protons.

In order to probe the possibility of CO insertion, INT B was heated for 44 hours, from 60°C-85°C. The ^{1}H NMR spectrum (Figure 3.12) showed that no change had occurred. Thus, CO insertion in the absence of alkyne did not occur, even at elevated temperatures.

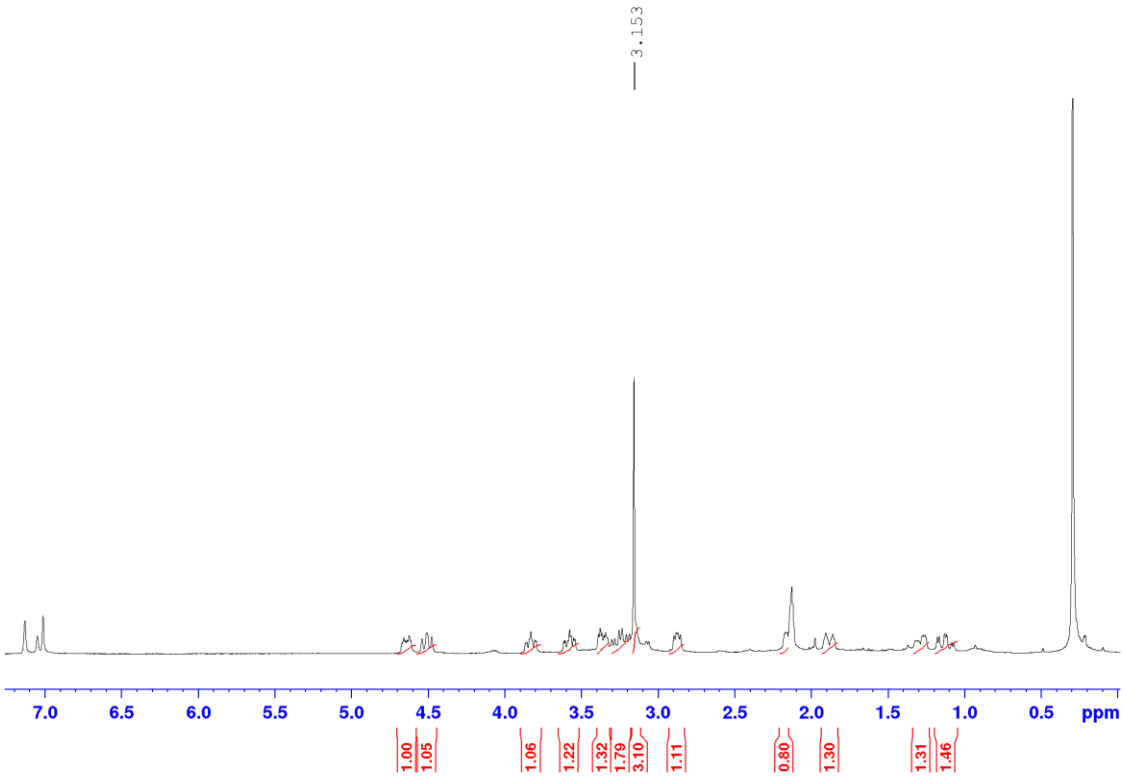

Figure 3.12: ^{1}H NMR (300 MHz, toluene-d_8) spectrum of INT B after 44 hours of heating at 60-85°C.

In the effort to ascertain if this complex was an intermediate in the [5 + 1 + 2 + 1] catalytic cycle, various alkynes were reacted with the intermediate. Upon the addition of 1 equiv. of phenylacetylene to 1 equiv. of INT B at room temperature, no reaction occurred, as shown by the ^{1}H NMR spectrum in Figure 3.13.

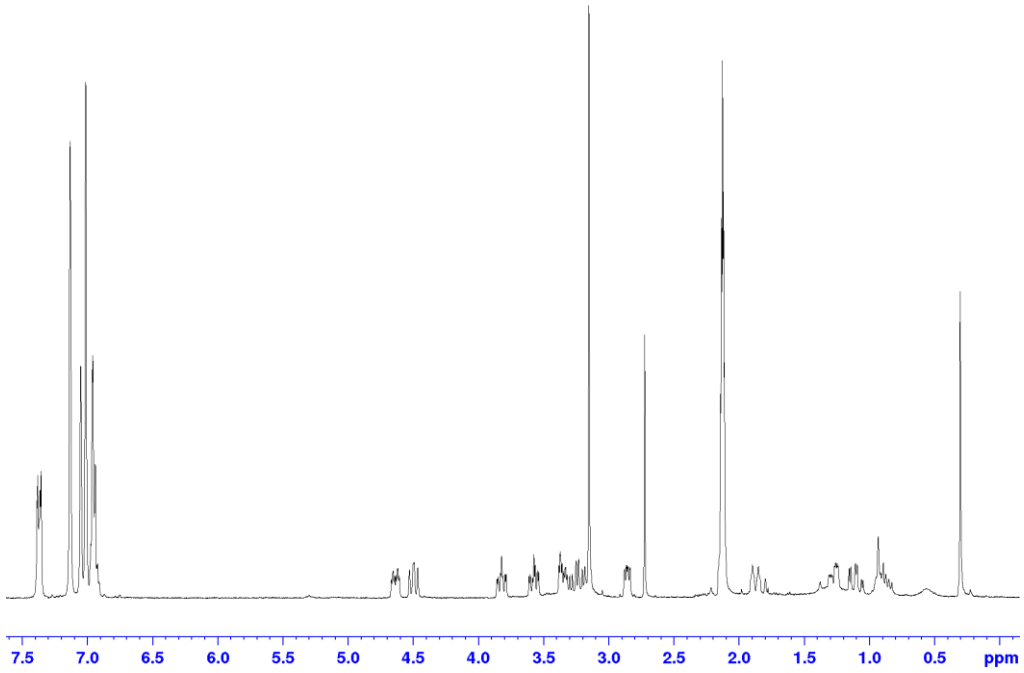

Figure 3.13: ^{1}H NMR (300 MHz, toluene-d_8) spectrum of INT B + phenylacetylene.

A ^{1}H NMR spectrum of the phenylacetylene-INT B solution obtained about 24 hours after addition of the alkyne (Figure 3.14), revealed that the alkyne changed in composition. However, this change was not a result of alkyne insertion into INT B, as Fig. 3.14 did not show a change in the multiplicities or chemical shifts of the INT B protons. Thus, a degradation of phenylacetylene or coordination to the metal centre of free catalyst might have caused this change. The sample was heated at 48°C for over 20 hours until degradation, without the observation of an insertion product.

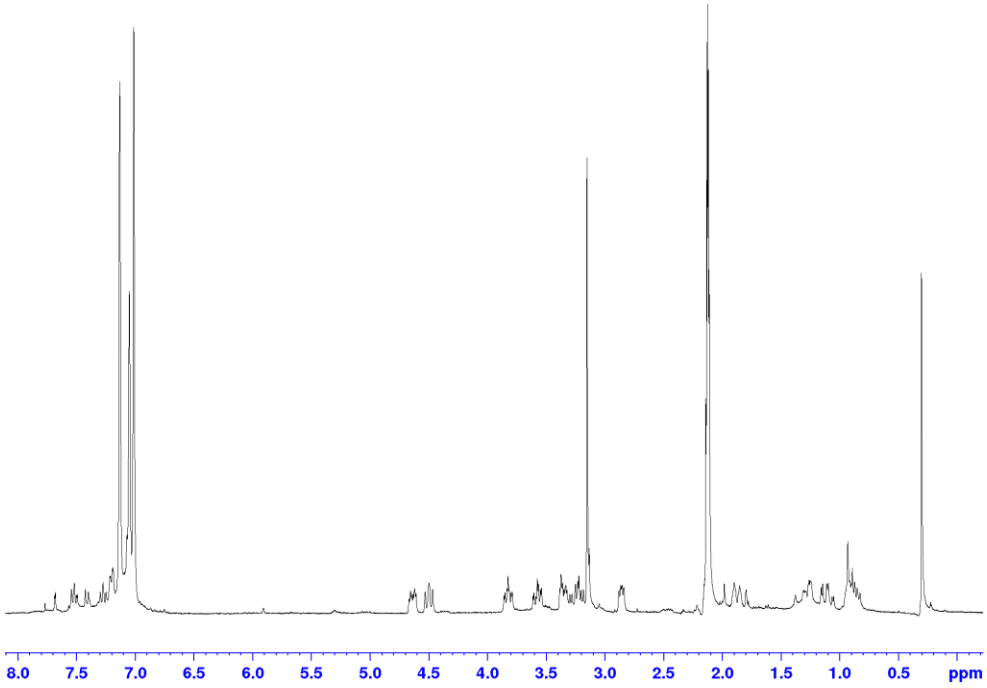

Figure 3.14: ^{1}H NMR (300 MHz, toluene-d$_8$) spectrum of INT B + phenylacetylene 24 hours after alkyne addition.

2 equiv. of 2-butyne were added to 1eq. of INT B at room temperature. After 24 hours, a ^{1}H-NMR spectrum (Fig. 3.15) showed that alkyne insertion into INT B had not occurred. Due to the low boiling point of 2-butyne, variable temperature studies were not carried on this sample for precautionary reasons.

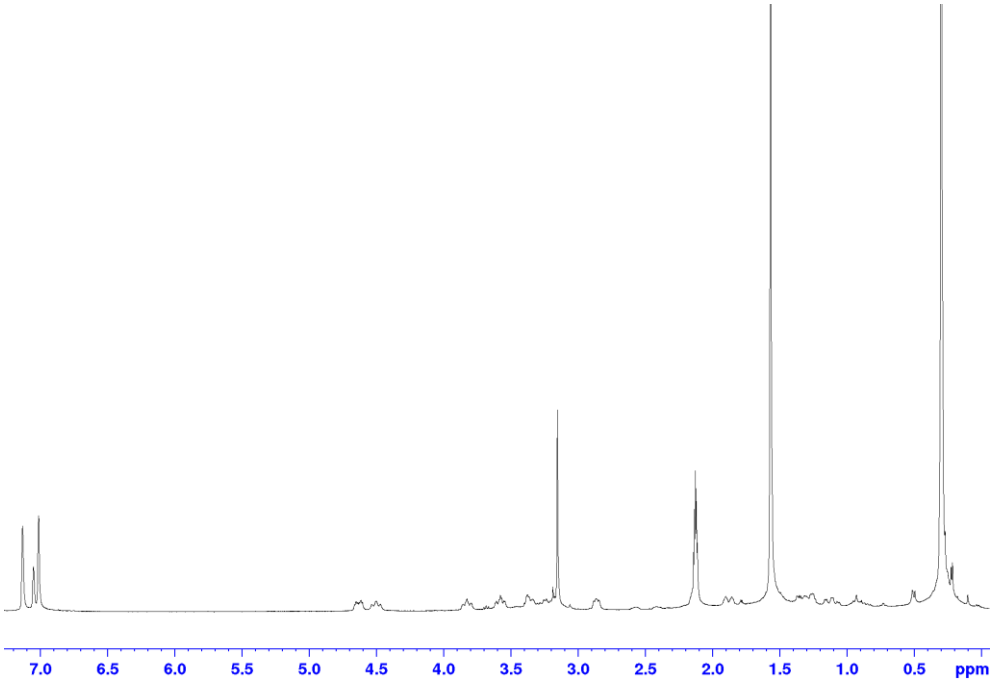

Figure 3.15: ^{1}H NMR (300 MHz, toluene-d$_8$) spectrum of INT B + 2-butyne 24 hours after alkyne addition.

When 1 equiv. of 4-ethynylbiphenyl was added to 1 equiv. of INT B, the ^{1}H NMR spectrum shown in Figure 3.16 was obtained. The multiplet at 7.33-7.15 ppm was due to the phenyl protons while the singlet at 2.82 ppm was due to the methine proton of the alkyne.

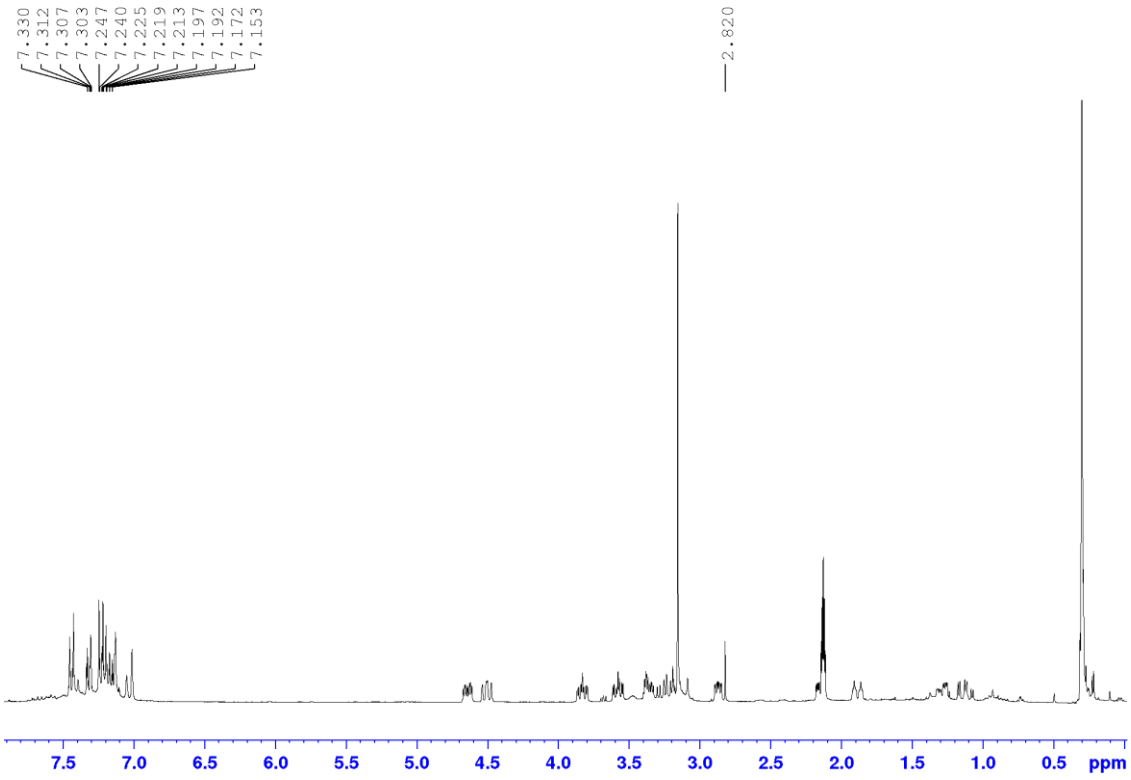

Figure 3.16: ^{1}H NMR (300 MHz, toluene-d$_8$) spectrum of INT B + 4-ethynylbiphenyl.

Upon heating this sample at 60°C for 74 hours, the obtained ^{1}H NMR spectrum (Figure 3.17) revealed a change in the alkyne structure, without a corresponding change in that of INT B. Thus, alkyne insertion into INT B did not occur. This structural change may have been due to alkyne degradation or coordination to the metal centre of free catalyst. Continuous heating at 90°C for an additional 40 hours, led to the formation of side products without a change in the proton signals of INT B.

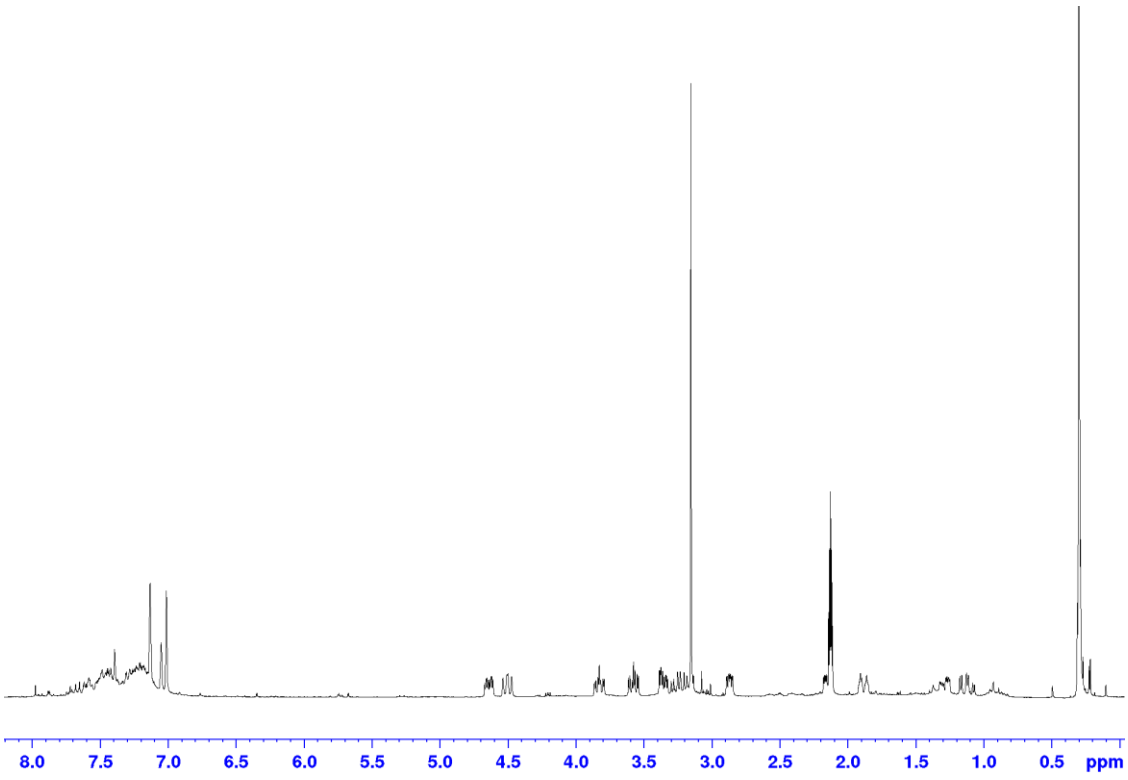

Figure 3.17: ^{1}H NMR (300 MHz, toluene-d_8) spectrum of INT B + 4-ethynylbiphenyl after heating at 60°C for 74 hours.

Computational investigations of Rh-catalysed [5 + 2] cycloadditions have revealed that the catalyst dimer, $[RhCl(CO)_2]_2$, monomerizes and loses CO to form the active species, RhCOCl.[31] In the synthesis of INT B, 0.5-1 equiv. of $[RhCl(CO)_2]_2$ was reacted with VCP in various runs. Thus, for these runs, the potential for the generation of 1-2 equiv. of either $Rh(CO)_2Cl$ or RhCOCl existed. This excess is thought to have hindered the progression of the respective reactions. Instances of the deleterious effect of excess metal catalyst loading have been reported. For example, in the $[RhCl(CO)_2]_2$ catalysed [5 + 2 + 1] cycloaddition of vinylcyclopropanes, CO and alkynes to yield bicyclo[3.3.0]octenones,[38] Wender reported that although lowering the catalyst loading led to longer reaction periods, higher yields were obtained in such instances. Thus, it is possible that the inability of excess Rh catalyst (1-2 equiv.) to promote the

cycloaddition studied herein, was due to production of an off-cycle species when $[RhCl(CO)_2]_2$ was used in excess.

To probe this idea and validate the necessity of a low catalyst concentration, 0.08 equiv. (8% mol loading) of $[RhCl(CO)_2]_2$ was reacted with 1 equiv. of VCP and 0.5 equiv. of 4-ethynylbiphenyl under CO (1 atm). An overlay of the resulting spectra upon mixing (blue), after 2 hours at 60°C (red) and after 16 hours at 60°C is shown in Figure 3.18.

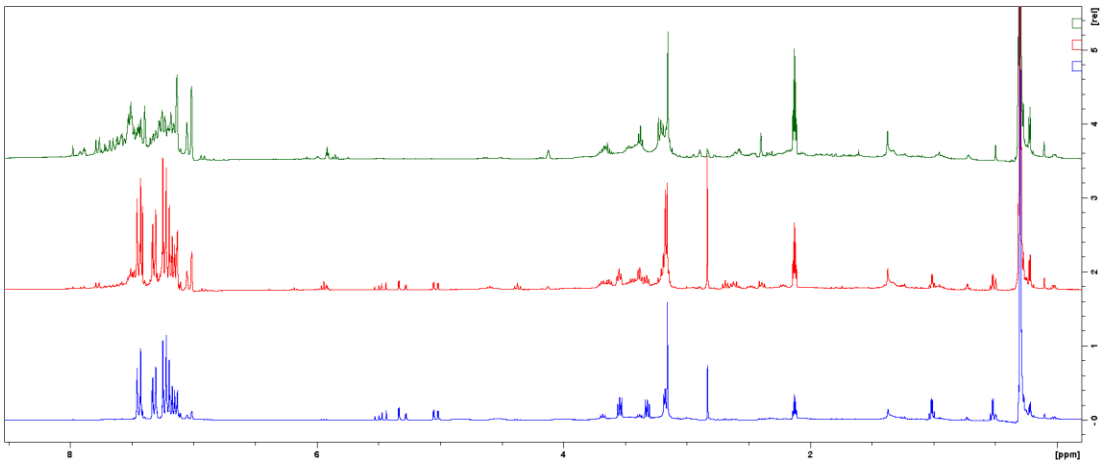

Figure 3.18: ^{1}H NMR (300 MHz, toluene-d_8) spectrum of catalyst + VCP + 4-ethynylbiphenyl, showing the chronological consumption of the starting materials.

From this Figure, it is evident that with time and the application of heat, the consumption of both 4-ethynylbiphenyl and VCP occur at 8% mol loading of $[RhCl(CO)_2]_2$. Thus, in contrast to trials where 0.5-1 equiv. of $[RhCl(CO)_2]_2$ failed to catalyse the reaction, this trial showed that a lower catalyst concentration was mandatory for reaction progression.

This necessity of low Rh concentration elicited the further study of INT B. To further probe if INT B was a part of the catalytic cycle, an aliquot was reacted with VCP and 4-ethynylbiphenyl under CO. The rationale for this action was to ascertain if INT B would be consumed along with the other reagents. If this occurred, then it is likely that

INT B is a part of the catalytic cycle. In addition, a low concentration of INT B was used, since it was shown that high Rh concentrations hindered the reaction. Thus, a volume of INT B in toluene-d_8 containing 8% mol of $[RhCl(CO)_2]_2$ was reacted with 1 equiv. of VCP and 1 equiv. of 4-ethynylbiphenyl under CO (1 atm). An overlay of the resulting spectra upon mixing (blue), after 13 hours at 35°C (red) and after an additional 5.5 hours at 45°C is shown in Figure 3.19.

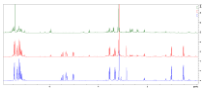

Figure 3.19: ^{1}H NMR (300 MHz, toluene-d_8) spectrum of INT B + VCP + 4-ethynylbiphenyl, showing the chronological consumption of the starting materials.

While Scheme 3.1 depicts this reaction, Figure 3.20 shows the spectrum obtained after an additional 5.5 hours of heating at 45 °C.

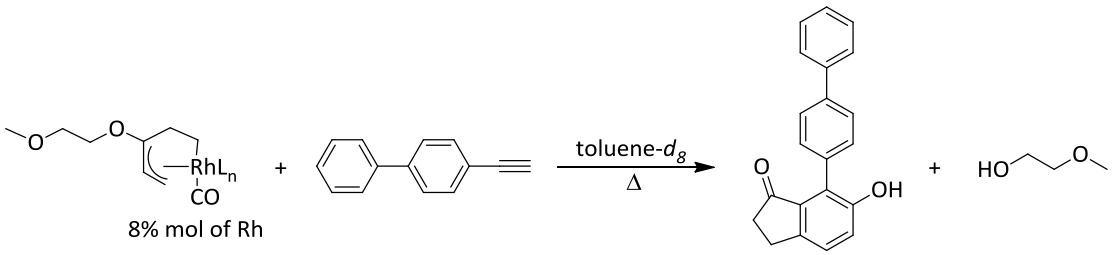

Scheme 3.1: Synthesis of hydroxydihydroindanone from INT B and 4-ethynylbiphenyl.

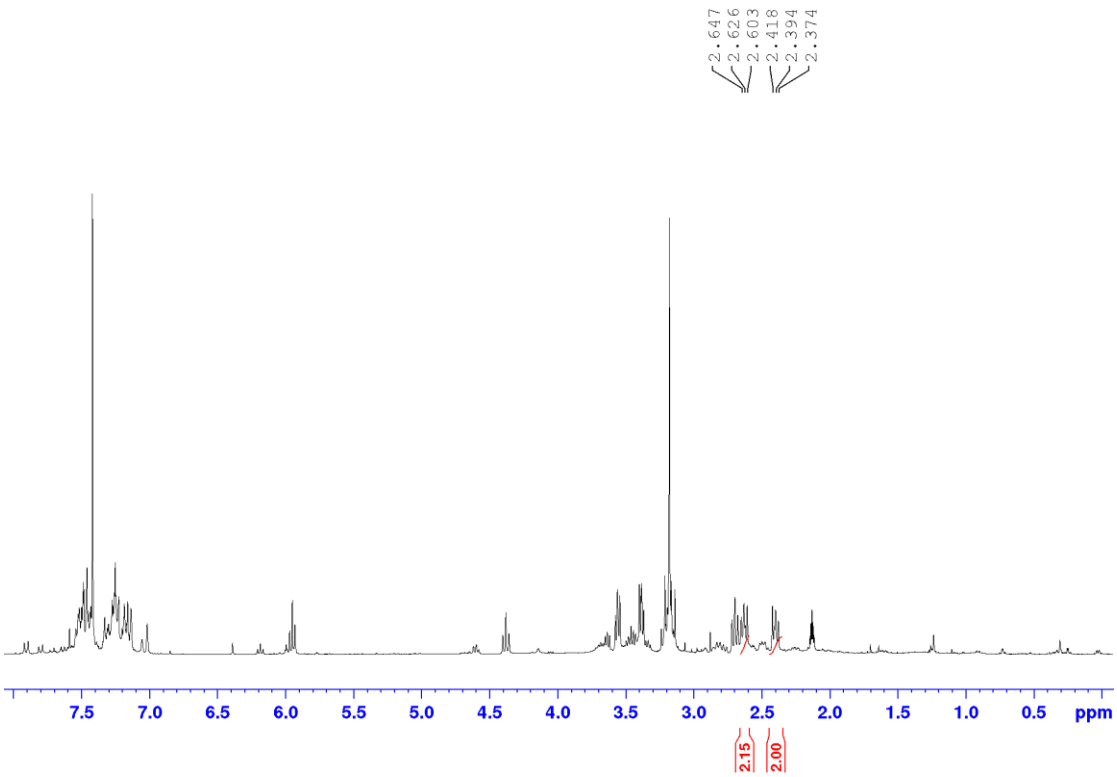

Figure 3.20: ^{1}H NMR (300 MHz, toluene-d_8) spectrum of INT B + VCP + 4-ethynylbiphenyl after 13 hours of heating at 35 °C and an additional 5.5 hours at 45 °C.

From Figure 3.20, the potential formation of hydroxydihydroindanone is apparent: the multiplets at 2.65-2.60 ppm and 2.42-2.37 ppm are indicative of indanone alkyl protons. Also, the change in the phenyl region (8.0-7.0 ppm) of this spectrum when compared to that of the initial (blue) spectrum in Figure 3.19, is indicative of the conversion of starting materials to the hydroxydihydroindanone. The other multiplets shown in Figure 3.20 are possibly due to by-products such as 2-methoxyethanol.

While the consumption of both VCP and alkyne is evident from the Figure 3.19, INT B was not spectroscopically observed (even at high magnifications of the blue spectrum) at the start of the reaction. Thus, INT B is likely an inactive species that is converted to an active species in excess solvent (lower concentration of the Rh-

catalyst). In addition, it is possible that this reaction was catalysed by either the active species, or free catalyst in the solution.

A mechanistic hypothesis for the formation of INT B is depicted in Scheme 3.2. The loss of 2 CO ligands from a Rh-centre of the catalyst dimer upon C-C bond activation of the VCP affords the 16-electron species, INT A. The coordination of 1 CO to the unsaturated Rh-centre of INT A affords the 18-electron species, INT B. While this coordination is facilitated by increasing CO concentration (achieved by bubbling CO into the solution), free CO displaced during C-C bond activation may also coordinate to the Rh-centre. Thus, the existence of INT A and INT B before CO addition, is possible. It is thought that the two methyl peaks seen in Fig. 3.7 is indicative of both species. However, bubbling CO into the solution favours the forward equilibrium step, towards the formation of INT B. This is likely why only one of both species is observed after bubbling CO through the solution. In this stable, inactive state, INT B is neither capable of facilitating CO insertion nor alkyne coordination. However, when an aliquot of INT B is transferred to a dilute CO infused solution containing less catalyst and more VCP, the monomerisation of INT B to INT C and $RhCl(CO)_2$ is facilitated. Computational investigations (Fig. 3.1) have shown that analogues of INT C result from CO-coordination. In addition, these investigations have also shown that the loss of CO from $RhCl(CO)_2$ yields the active catalyst, RhClCO. Thus, both products of monomerisation readily enter the cycle to catalyse the formation of the hydroxydihydroindanone.

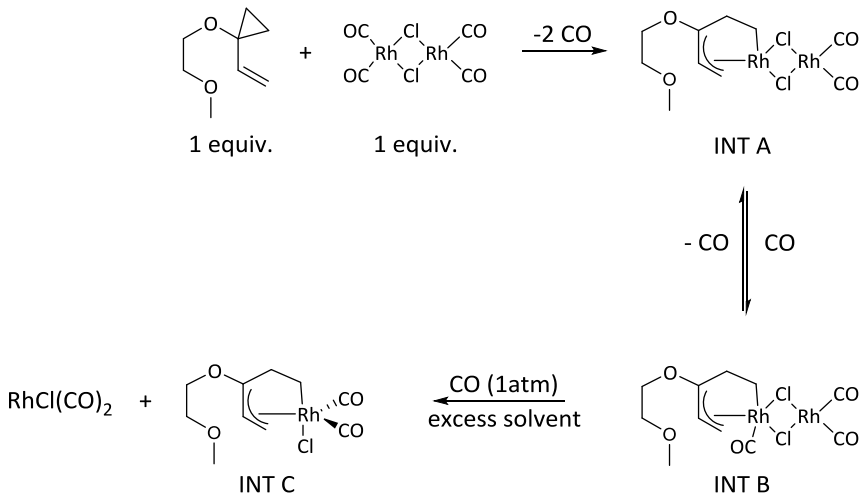

Scheme 3.2: Hypothesised mechanism for the formation of INT B.

4. Conclusion

The spectroscopic investigation reported herein probed the reaction mechanism of the Rh-catalysed [5 + 1 + 2 + 1] cycloaddition reaction. In accordance with the aim of this research, part of the molecular structure of an intermediate was identified. While this inactive species is readily formed in the presence of excess catalyst, it converts to an active species at lower Rh concentrations. In addition, it was also determined that excess catalyst loading is detrimental to the cycloaddition reaction as this inactive intermediate mitigates CO and alkyne insertion. A shortcoming of this research, is the inability to detect computationally predicted intermediates via the spectroscopic techniques employed. In addition, since reactions were done on NMR scale, the purification of any products proved futile. Thus, the consumption of starting materials as well as the appearance of new NMR signals were the only indications of reaction progression.

5. Future Work

The characterisation of INT B will be continued via other techniques. It is important to determine the complete structure of this compound, as the mechanism involving the conversion from the inactive to active form can then be corroborated. By performing ^{103}Rh NMR experiments at the different reaction stages, the changes in the chemical shift of Rh will further highlight the nature of the inactive species. Thus, the conversion of two isomers to one upon the addition of CO (Figs. 3.7 and 3.8) will be monitored via changes in the respective ^{103}Rh NMR spectra. In addition, ^{103}Rh NMR experiments will be conducted on a sample containing the active species (obtained when INT B is added to an excess, CO infused solution). These studies will highlight the changes that occur in the conversion of the inactive to the active species. Infrared spectroscopy will also be employed in the characterisation of INT B. By monitoring the changes that occur in the carbonyl region of the spectrum, insights into the structures of these intermediates will be gained.

The pursuit of crystal growth will continue, as x-ray crystallography will solve the structure of the inactive species. In addition, mass spectrometry will be used to ascertain the molecular weight of this species, in the effort to determine its molecular structure.

A computational investigation that probes possible products formed after CO coordination to INT B, will also be performed.

Upon the characterisation of INT B and other intermediates that result from CO and alkyne insertion, the reaction kinetics and rate laws governing this reaction will be investigated.

6. References

1. (a) Katritzky, A. R.; Dennis, N. *Chem. Rev.* **1989**, 89, 827. (b) Gothelf, K. V.; Jorgensen, K. A. *Chem. Rev.* **1998**, 98, 863. (c) Goodall, G. W.; Hayes, W. *Chem. Soc. Rev.* **2006**, 35, 280. (d) Ylijoki, K. E. O.; Stryker, J. M. *Chem. Rev.***2013**, *113*, 2244.
2. Diels, O.; Alder, K. *Ann*. **1928**, 460, 98.
3. Lautens, M.; Klute, W.; Tam, W. *Chem. Rev*. **1996**, 96, 49.
4. *Modern Rhodium Catalyzed Organic Reactions*; Evans, P. A., Ed.; Wiley-VCH: New York, 2005
5. Doyle, M. P.; Griffin, J. H.; Bagheri, V.; Dorow, R. L. *Organometallics* **1984**, 3, 53.
6. Doyle, M. P. *Chem. Rev*. **1986**, 86, 919.
7. Salomon, R. G.; Salomon, M. F.; Heyne, T.R. *J. Org. Chem.* **1975**, 40(3), 756.
8. Padwa, A.; Krumpe, K. E.; Gareau, Y.; Chiacchio, U. *J. Org. Chem*. **1991**, 56, 2523.
9. Shibata, T.; Takami, K.; Kawachi, A. *Org. Lett.* **2006**, 8, 1343.
10. Simmons, H. E.; Smith, R. D. J. Am. Chem. Soc. 1958, 5323
11. (a) Pirrung, M. C.; Zhang, J.; McPhail, A. T. *J. Org. Chem*. **1991**, 56, 6269. (b) Pirrung, M. C.; Zhang, J.; Lackey, K.; Sternbach, D. D.; Brown, F. *J. Org. Chem*. **1995**, 60, 2112.
12. Alonso, M. E.; Morales, A.; Chitty, A. W. *J. Org. Chem*. **1982**, 47, 3747.
13. Wender, P. A.; Paxton, T. J.; Williams, T. J. *J. Am. Chem. Soc.* **2006**, 128, 14814.
14. (a) Ojima, I.; Tzamarioudaki, M.; Li, Z.; Donovan, R. J. *Chem. Rev.* **1996**, 96, 635. (b) Nakamura, I.; Yamamoto, Y. *Chem. Rev*. **2004**, 104, 2127.
15. Koga, Y.; Kobayashi, T.; Narasaka, K. *Chem. Lett*. **1998**, 27, 249.
16. Jeong, N.; Lee, S.; Sung, B. K. *Organometallics* **1998**, 17, 3642.
17. Kim, H. J.; Song, T.; Chung, Y. K. *Org. Lett.* **2017**, 19, 1248.

18. Murakami, M.; Itami, K.; Ito Y. *Organometallics* **1999**, 18, 1326.

19. Mizuno, A.; Kusama, H.; Iwasawa, N. *Angew. Chem. Int. Ed.* **2009**, 48, 8318.

20. (a) Grigg, R.; Scott, R.; Stevenson, P. *Tetrahedron Lett*. **1982**, 23, 2691. (b) Neeson, S. J.; Stevenson, P. J. *Tetrahedron Lett.* **1988**, 29, 813. (c) Neeson, S. J.; Stevenson, P. J. *Tetrahedron* **1989**, 45, 6239.

21. Grigg, R.; Scott, R.; Stevenson, P. *J. Chem. Soc., Perkin Trans. 1* **1988**, 1357.

22. (a) Colman, J. P.; Hegedus, L. S. *Principles and Applications of Organotransition Metal Chemistry; University Science Books*: Menlo Park, 1980 (b) Vollhardt, K. P. C. *Angew. Chem., Int. Ed. Engl.* **1984**, 23, 539.

23. Matsuda, I.; Shibata, M.; Sato, S.; Izumi, Y. *Tetrahedron Lett*. **1987**, 28, 3361.

24. Wender, P. A.; Jenkins, T. E.; Suzuki, S. *J. Am. Chem. Soc*. **1995**, 117, 1843.

25. Jolly, R. S.; Luedtke, G.; Sheehan, D.; Livinghouse, T. *J. Am. Chem. Soc*. **1990**, 112, 4965.

26. Wender, P. A.; Jenkins, T. E. *J. Am. Chem. Soc*. **1989**, 111, 6432.

27. Brancour, C.; Fukuyama, T.; Ohta, Y.; Ryu, I.; Dhimane, A-L.; Fensterbank, L.; Malacria, M. *Chem. Commun.* **2010,** 46, 5470.

28. Kozubek, A.; Tyman, J. H. P. *Chem. Rev*., **1999**, 99, 1.

29. Ke, X-N.; Schienebeck, C. M.; Zhou, C-C.; Xu, X-F.; Tang, W-P. *Chin. Chem. Lett*. **2015**, 26, 730.

30. Wender, P. A.; Takahashi, H.; Witulski, B. *J. Am. Chem. Soc.* **1995**, 117, 4720.

31. (a) Yu, Z-X.; Wender, P. A.; Houk, K. N. J. Am. Chem. Soc. 2004, 126, 9154. (b) Yu, Z.-X.; Cheong, P. H.-Y.; Liu, P.; Legault, C. Y.; Wender, P. A.; Houk, K. N. *J. Am. Chem. Soc*. **2008**, 130, 2378. (c) Liu, P.; Cheong, P. H.-Y.; Yu, Z.-X.; Wender, P. A.; Houk, K. N. *Angew. Chem*., *Int. Ed*. **2008**, 47, 3939.

32. Hong, X.; Liu, P.; Houk, K. N. *J. Am. Chem. Soc*. **2013**, 135, 1456.

33. Hong, X.; Trost, B. M.; Houk, K. N. *J. Am. Chem. Soc*. **2013**, 135, 6588.

34 Reddy, R. P.; Davies, H. M. L. *J. Am. Chem. Soc.* **2007**, 129, 10312.

35. Krainz, T.; Chow, S.; Korica, N.; Bernhardt, P. V.; Boyle, G. M.; Parsons, P. G.; Davies, H. M. L.; Williams, C. M. *Eur. J. Org. Chem*. **2016**, 41.

36. Wender, P. A.; Correa, A. G.; Sato, Y.; Sun, R. *J. Am. Chem. Soc.* **2000**, 122, 7815.

37. Huffman, M. A.; Liebeskind, L. S. *J. Am. Chem. Soc*. **1993**, 115, 4895.

38. Wender, P. A.; Gamber, G. G.; Hubbard, R. D.; Zhang, L. *J. Am. Chem. Soc*. **2002**, 124, 2876.

39. Wang, Y.; Yu, Z-X. *Acc. Chem. Res*. **2015**, 48, 2288.

40. Wender, P. A.; Christy, J. P. *J. Am. Chem. Soc.* **2006**, 128, 5354.

41. Wender, P. A.; Gamber, G. G.; Hubbard, R. D.; Pham, S. M.; Zhang, L. *J. Am. Chem. Soc.* **2005**, 127, 2836.

42. Frédérick, R.; Dumont,W.; Ooms, F.; Aschenbach, L.; Van der Schyf, C. J.; Castagnoli, N.; Johan Woutersa, J.; Kriefc, A. *J. Med. Chem*. **2006**, 49, 3743.

43. Chanda, D.; Bhushan, S.; K. Guru, S. K.; Shanker, K.; Wani, Z. A.; Rah, B. A.; Luqman, S.; Mondhe, D. M.; Pal, A.; Negi, A. S. *Eur. J. Pharm. Sci.* **2012,** 47, 988.

44. Finkielsztein, L. M.; Castro, E. F.; Fabián, L. E.; Moltrasio, G. Y.; Campos, R. H.; Cavallaro, L. V.; Moglioni, A. G. *Eur. J. Med. Chem.* **2008**, 43, 1767.

45. Chai, J-D.; Head-Gordon, M. *Phys. Chem. Chem. Phys*. **2008**, 10, 6615.

46. (a) Weigend, F.; Ahlrichs, R. *Phys. Chem. Chem. Phys*. **2005**, 7, 3297. (b) Weigend, F. *Phys. Chem. Chem. Phys*. **2006**, 8, 1057.

47. Frisch, M. J.; *et al.* Gaussian, Inc., Wallingford CT, **2010**.

48. Von Philipsborn, W. *Chem. Soc. Rev*. **1999**, 28, 95.

49. Zakzeski, J.; Burton, S.; Behn, A.; Head-Gordon, M.; Bell, A. T. *Phys. Chem. Chem. Phys.* **2009,** 11, 9903.

50. Dauben, H. J. Jr.; McCoy, L. L. *J. Am. Chem. Soc.*, **1959**, 81, 4863.

51 . Smith, R. D.; Simmons, H. E. *Org. Synth*. **1961**, 41, 72.

52. Wender, P. A.; Dyckman, A, J.; Husfeld, C. O.; Scanio, M. J. C. *Org. Lett*. **2000**, 2, 1609.

53. This computational investigation was performed by Mbaezue I. I. and Prof. K. E. O. Ylijoki. While the computational study is not a product of this thesis, it noteworthy to mention its relevance to the spectroscopic investigations reported herein.

54. Fulmer, G. R.; Miller, A. J. M.; Sherden, N. H.; Gottlieb, H. E.; Nudelman, A.; Stoltz, B. M.; Bercaw, J. E.; Goldberg, K. I. *Organometallics* **2010**, 29, 2176.

7. Appendix

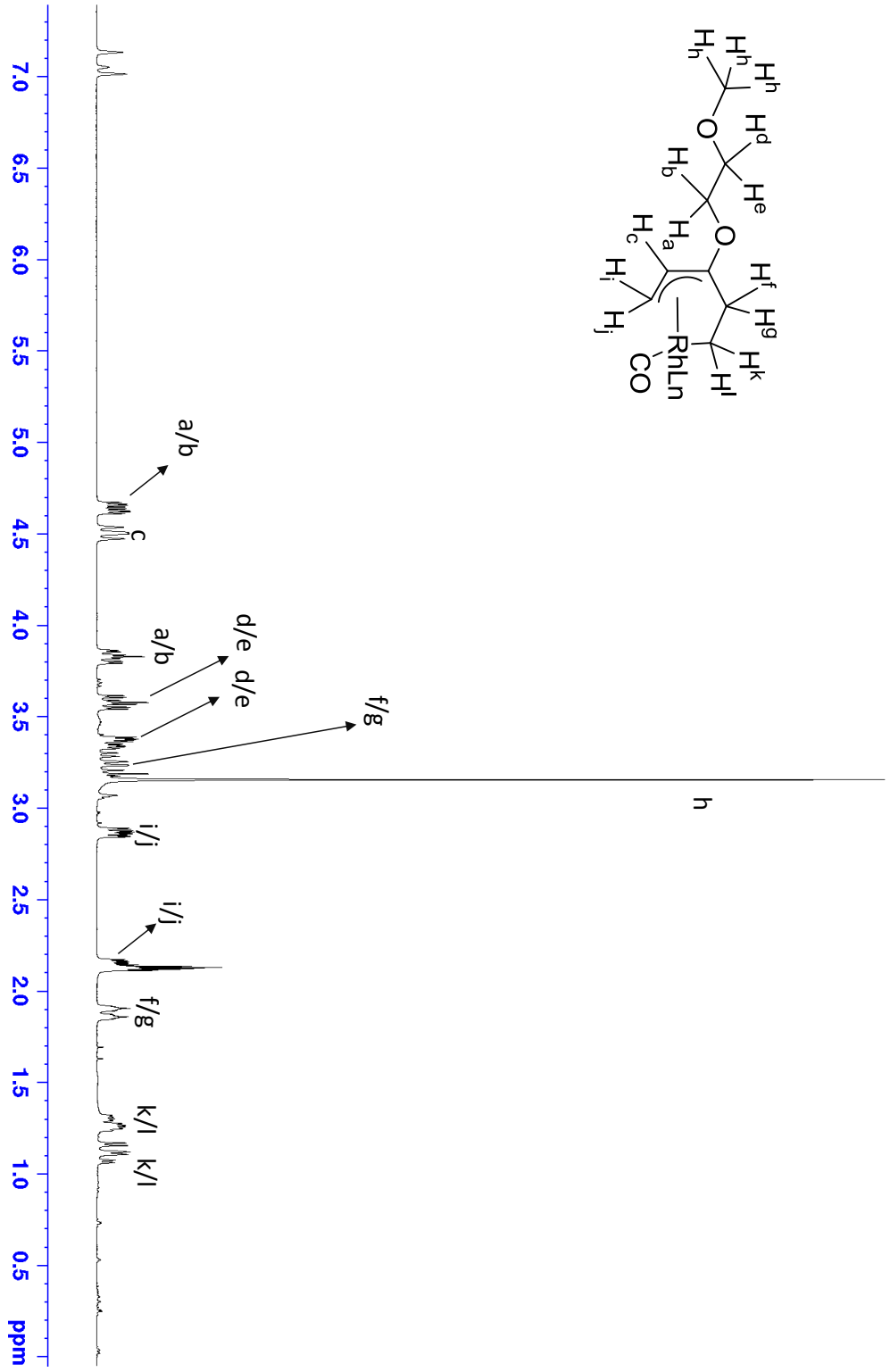

Figure 7.1: Proton assignments of INT B.

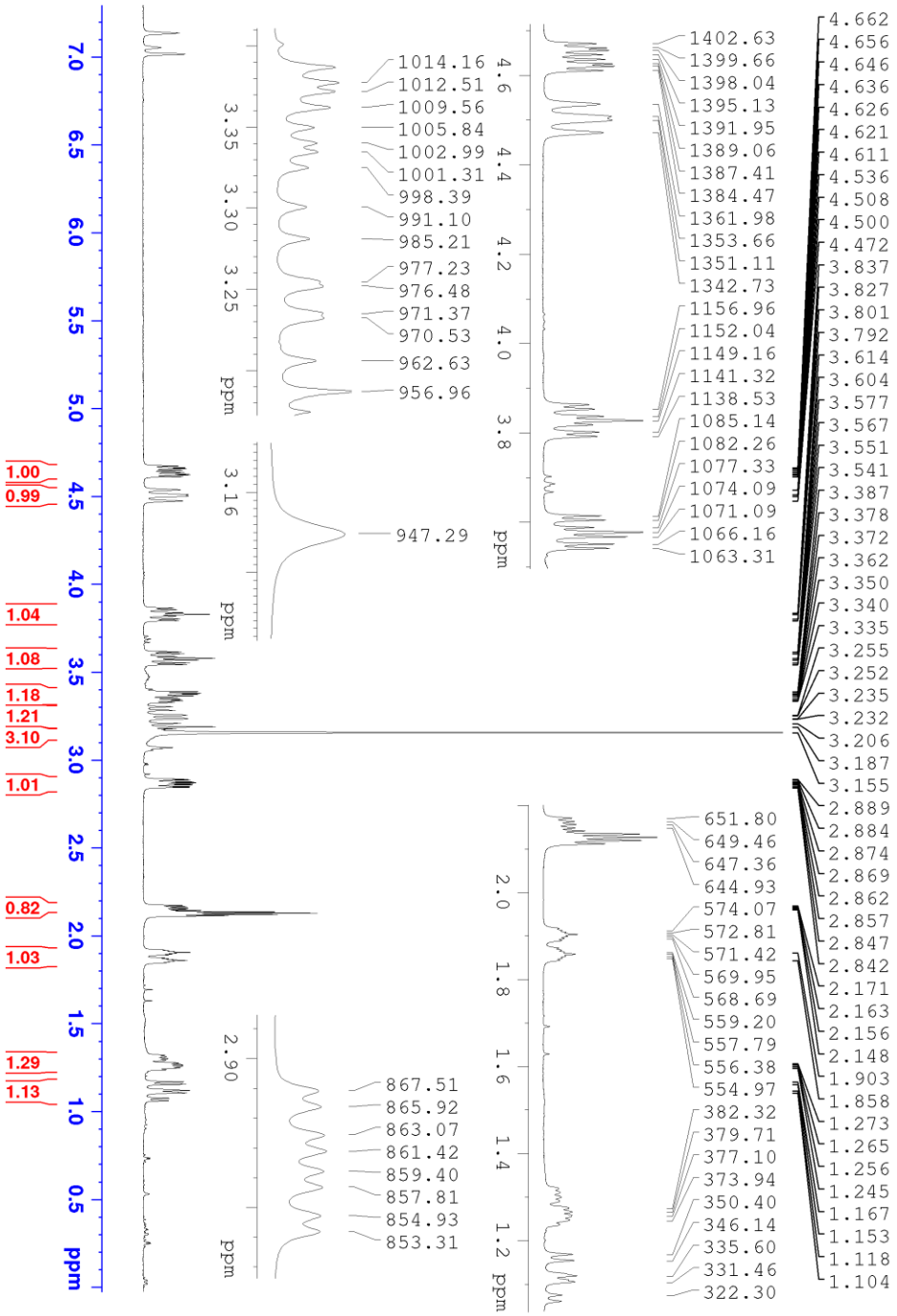

Figure 7.2: ^{1}H NMR (300 MHz, toluene-d_8) spectrum of INT B showing relevant peaks and frequencies.

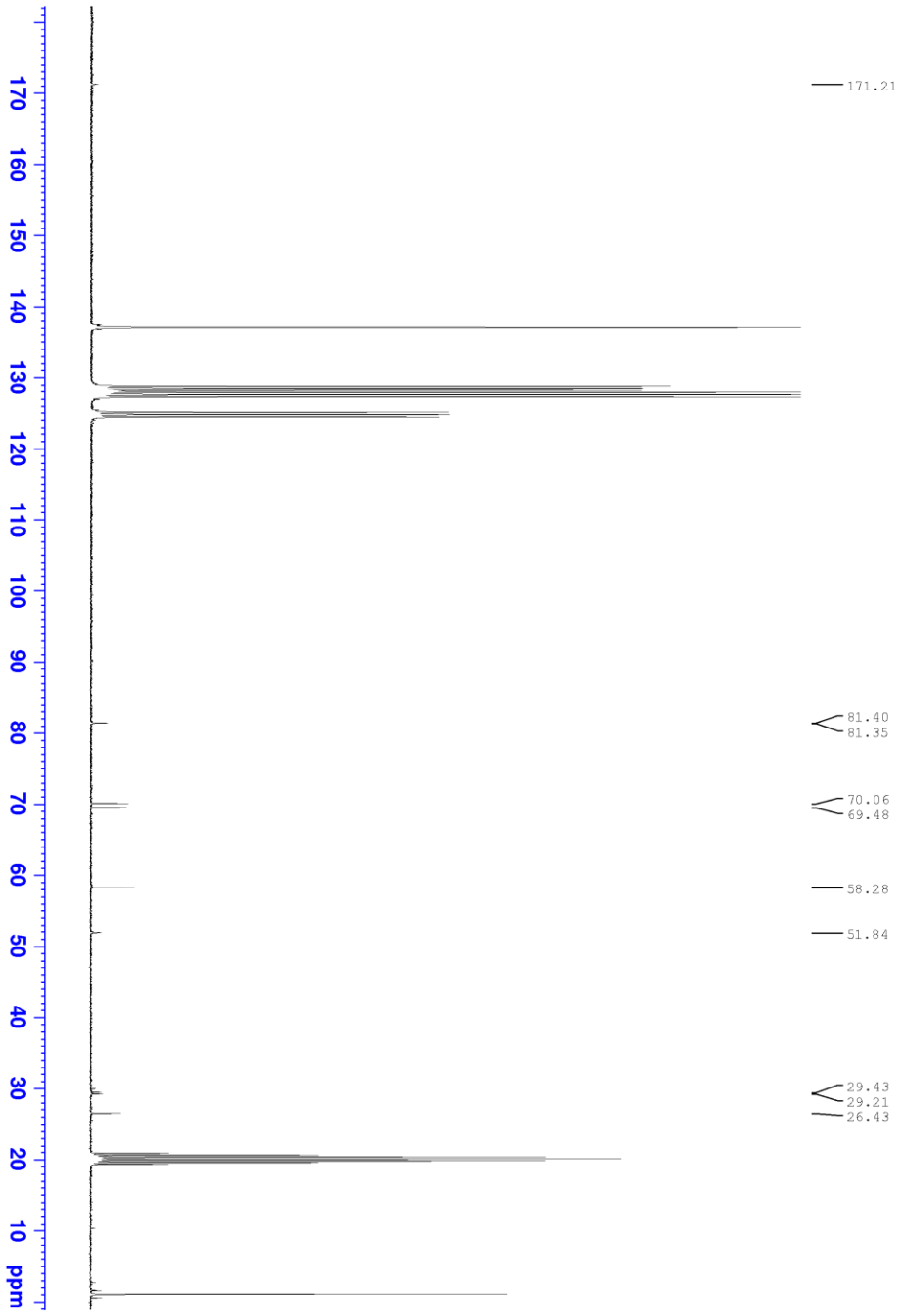

Figure 7.3: ^{13}C NMR (75 MHz, toluene-d_8) spectrum of INT B showing the chemical shifts of relevant peaks.

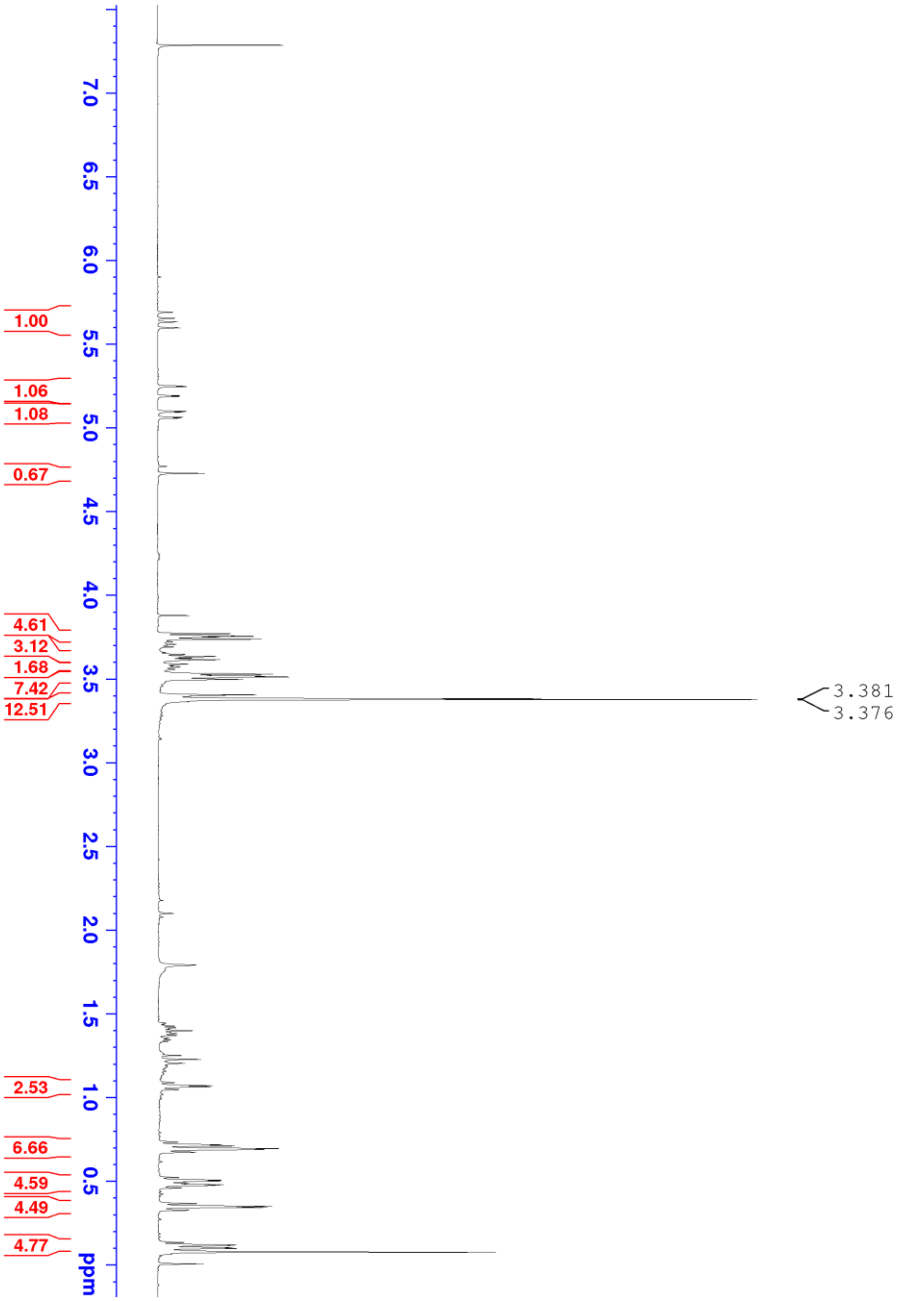

Figure 7.4: ^{1}H NMR (300 MHz, $CDCl_3$) spectrum showing the product mixture of VCP and the double cyclopropanation compound.